IEEE Access
Multidisciplinary | Rapid Review | Open Access Journal

Received August 22, 2021, accepted September 8, 2021, date of publication September 10, 2021,
date of current version September 21, 2021.

Digital Object Identifier 10.1109/ACCESS.2021.3111957

Graph Synthesis for Pig Breed Classification From Muzzle Images

SHOUBHIK CHAKRABORTY[1], KANNAN KARTHIK[1], AND SANTANU BANIK[2]
[1]Department of Electronics and Electrical Engineering, Indian Institute of Technology Guwahati, Guwahati, Assam 781039, India
[2]Animal Genetics and Breeding, ICAR-National Research Centre on Pig, Guwahati, Assam 781015, India

Corresponding author: Shoubhik Chakraborty (shoubhik@iitg.ac.in)

This work involved human subjects or animals in its research. The authors confirm that all human/animal subject research procedures and protocols are exempt from review board approval.

ABSTRACT Non-intrusive and automated detection of pig breeds, particularly from visual standpoint, is important from a food quality tracking perspective. In this work, colour as well as texture based visual descriptors from muzzle images have been identified, which, serve as breed-identifiers to separate four common pig-breeds: Duroc, Ghungroo, Hampshire and Yorkshire. While these handcrafted visual descriptors by themselves are fairly robust and discriminative, it is recognized that by controlling the decision space by choosing the feature-type based on colour or texture or both and the order in which particular breeds are siphoned, classification accuracy can be improved considerably. In that light, a stable, relatively data-independent, breed-specific, hierarchical tree synthesis and feature selection procedure is proposed based on a breed-pair cluster separation table. The proposed approach has been compared with the state of the art Phylogenetic distance based Hierarchical Agglomerative Clustering algorithm (AGNES) and also with the standard decision tree classification algorithm. On cross-validation, When completely different sets of pigs were used for training and testing (50-50 split), the proposed algorithm reported relatively high mean classification accuracies of 86.45% for Duroc, 93.02% for Ghungroo, 86.91% for Hampshire and 98.54% for Yorkshire, respectively.

INDEX TERMS Pig breeds, Gradient Significance Map, morphological top hat operator, colour histogram, graph synthesis, DGau filter.

I. INTRODUCTION

Animal biometrics, particularly of a visual type [1], [2], play an important role in tracking down animals, which have significant commercial value. While some animals are important from an individual standpoint, some assume an importance from a breed perspective. The term 'breed', is defined as a specific class of animals exhibiting some similarities in morphological or physiological traits, which have been propagated over generations, due to inheritance of some common gene-pool by descent.

For domesticated animals, such as cows, goats and pigs, whose ''produce'', in some form or the other is consumed (i.e. has commercial value and impact), the identity of the cow or pig in a larger group context, i.e. its breed-type, becomes crucial. For instance, it has been found and recorded that the following four specific breeds of cows viz. Gir cow of Gujarat; Rathi cow of states Uttar Pradesh, Madhya Pradesh and Haryana; Red Sindhi cow of states Punjab, Haryana, Karnataka; Sahiwal cow of states Uttar Pradesh, Haryana and Madhya Pradesh, produce more than 50 litres of nutritious milk every day [3]. In the same vein, in the context of pigs, most farms prefer pure-breeds as opposed to cross-breeds from the point of view of reproduction and pork quality. Aspects connected to their natural health condition in current local environments, weight and size associated with specific pig-breeds, play a crucial role in formulating a preference for certain breed-types over others. The Large White Yorkshire, Hampshire, Duroc etc., are among the few imported exotic breeds in India [4]. The Yorkshire breed for instance is popular because it lends itself to cross-breeding. Being a prolific breeder, it provides a good amount of meat for consumption. Hampshire hogs on the other hand are noted for being well-muscled and rapid growers, and for exhibiting good carcass quality when used as meat animals.

The associate editor coordinating the review of this manuscript and approving it for publication was Zhan-Li Sun.

Most biometrics are found concentrated near sensory interfaces e.g. muzzle of pig [5] or facial profile in cows [1] or hoof patterns in horses. Aggregates of these biometric traces at a macro level, may qualify as what are known as ''breed identifiers''. For instance, the face, which is a crucial biometric from a social standpoint of human beings, can be analyzed at a coarser level involving colour, texture, facial feature skewness/bias, to segregate people hailing from different types of ethnic communities. These facial parameters are transmitted from generation to generation, as long as the ethnic group stays insular. In a similar fashion in the case of pigs, for a particular set of morphological parameters to qualify as a breed indicator the following conditions must be satisfied:

- There must be a biometric connection, i.e. these morphological parameters must be linked to their ancestors.
- Furthermore, these parameters should be concentrated near sensory interfaces, at places where there is a continuous interaction with the surrounding environment. Over generations some of these macro-morphological parameters will be ironed out and shall stabilize to be eventually passed down to future generations.

However, when it comes to the practical deployment of a breed profiling procedure, it is important to first identify the domain (visual, acoustic, chemical etc.), and then the nature of the measurements taken in that domain, which may qualify as breed-relevant features or statistics.

There are procedures for individual identification of animals, some intrusive and some non-intrusive. Intrusive methods such as ear notching and tagging, use of RFID tags etc, are often painful for the animals. Non-intrusive methods, however, based on images of certain parts of the body, such as auricular vein patterns in goats and pigs [6], have gained considerable attention from researchers. However, very few methods exist for breed identification of animals purely based on images. Some exemplar work related to dog-breed classification linked to biometrics of the visual type, can be found in Raduly *et al.* [7] and Kumar *et al.* [8], using deep neural networks.

Biometrics of the visual type can therefore be adapted and modified to generate breed descriptors in the visual domain for isolating and detecting breeds of a particular type. In this work, still images of faces of pigs or parts of the face, such as the tip of the snout (termed as the muzzle), have been found to be stable, yet discriminative visual identifiers, across breeds [5]. The main aim of this work is to check and establish whether the image of the muzzle of a pig qualifies as a robust breed identifier for four popular breeds viz. Duroc, Ghungroo, Hampshire and Yorkshire. The main contributions in this paper encompass the following fields:

- Segmentation of muzzle region from background: Design of a spatial filter for contour detection and contour interior cleaning. This is built on the principles of the dual-mode Gabor filter [9] with a conjoined operation of three Gabor variants along three different directions: 0^0, 120^0 and 240^0 each of which performs low pass filtering along one direction and differentiation along the other orthogonal direction.
- Selection of unique and customized secondary statistics for color descriptors such as the Sarle's index [10] for picking up dual colouration, on the muzzle particularly in the case of Hampshire and in some cases, even Duroc. On another front, eigen-decomposition performed in the $C_b - C_r$ space was used for characterizing the footprint of the 2D histogram.
- Graph synthesis for generating breed siphoning order: Feature selection was merged in a unique way with the tree construction procedure. Based on a baseline table containing pairwise distances across breed features and feature-specific cumulative distance analysis, a stable tree was created for each training set with 'selective' feature types being deployed at different decision points (or nodes in the tree).

A. BREED IDENTIFICATION AND IDENTIFIERS

It was surmised in an earlier work [5], that biometric identifiers tend to be concentrated near sensory interfaces. These sensory interfaces could be the eye (ocular type with the biometric in question being the iris), the ear (aural type dealing with vein patterns in the inner surface), the nose or snout (nasal and tactile type especially for pigs, involving the muzzle) and many others. While a single biometric identifier imparts a distinct identity to a particular pig, it does not directly qualify the pig in a larger group (analogous to ''race'' based classification for humans based on their origin and life-style over generations). When several biometric micro-identifiers are aggregated, at a coarser level they constitute what can be called a ''breed-identifier'', which qualifies the pig in a larger setting based on some similarities in traits.

The nasal disc on the snout of the pig, while being rigid enough to be used for digging, has numerous sensory receptors. Pigs tend to use their snout while exploring and searching for food items, to push objects, to flatten them, for scooping and for leveraging out thick roots. Furthermore, under natural conditions, pigs may spend 75% of their daily activity engaged in rooting and foraging [11]. Apart from this, the snout also houses the nasal interface carrying two nostrils as shown in Fig. 1, which plays a crucial role on several fronts such as: (i) Breathing, (ii) Discriminating between odors and tracking down food, (iii) Using the odors stemming from chemical discharges to locate one's mate [11], etc. This frontal portion or disk is termed as the ''muzzle''. Thus, the muzzle segment serves as both a tactile as well as a nasal interface for interacting with the environment. Owing to the presence of many sensory features in virtually the same location, it was concluded in an earlier work [5], that the frontal image of the muzzle covering the heart shaped nasal disc which houses two nostrils could be used as a ''breed identifier''. The pigs selected for analysis and profiling in this paper have crossed what is known as the weaning period (more than six weeks from the date of birth). This implies

TABLE 1. Distinguishing visual parameters from the original cropped muzzle colour images (taken from male pigs) and their corresponding GSMs.

	Duroc	Ghungroo	Hampshire	Yorkshire
Colour profile	Either completely powdery-black or Dual-coloured (pink and powdery-black with a slight white-tuft)	Greyish black	Dual coloured (pink and grey)	Pink
Texture profile	Dot pattern density high (only over powdery-black patch)	Dot density high virtually throughout the muzzle	Dot pattern density moderate (only over greyish segment of the muzzle)	Dot pattern density uniformly low over the entire muzzle

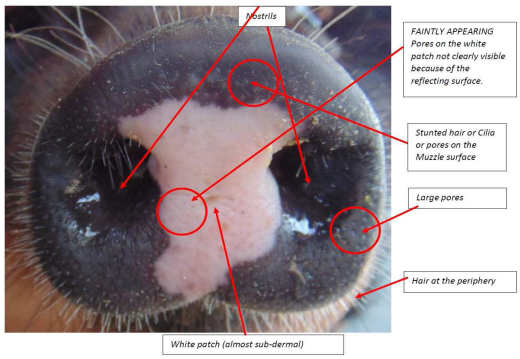

FIGURE 1. Description of the muzzle of a Duroc pig.

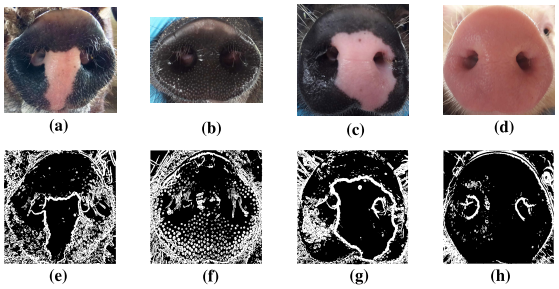

FIGURE 2. Pig muzzle imprints and the corresponding GSMs [2].

that their biometrics and breed-identities have crystallized morphologically in time. Beyond this weaning period virtually no change is observed in the biometric and breed-parameters [12].

The manually cropped muzzle segment of a Duroc pig is shown in Fig. 1 in which the key parts of a muzzle are marked. Apart from having two large nostrils and hair at the periphery of the muzzle contour, the muzzle region also shows large sweat pores and some stunted hair. This stunted hair was restricted to the darker region leaving the pinkish-white patch barren with respect to the hair. Sweat pores, however, were present uniformly in both the dark and pinkish white patches. Shown in Fig. 2(a-d) are the muzzle images corresponding to four different breeds: Duroc, Ghungroo, Hampshire and Yorkshire. By using a suitable texture processing mechanism based on gradients such as the Gradient Significance Map (GSM) [2] certain elements linked to the pores, hair and pinkish white patch (if present) on the muzzle surface can be emphasized or enhanced and brought out in the form of a binary map. The white portions in this GSM binary map, correspond to parts of the muzzle, which have some significance, as far as their connection with positions of the sweat-pores, hair and stunted hair are concerned. The following patterns can be discerned from the colouration profile seen in the original muzzle images in Fig. 2(a-d) and the texture profile from the GSMs computed in Fig. 2(e-h), covered in Table. 1. It is clear from Table. 1 that while examining breed-differences in a pairwise fashion, Ghungroo and Yorkshire turn out to be antipodes both with respect to colour and texture. However, because of the dual-colouration which prevails in the case of both Duroc and Hampshire pigs, the breed classification problem becomes tricky.

The rest of the paper is organized as follows: The muzzle segmentation procedure is discussed in Section. II. The customized visual descriptor selection procedure, signal-conditioning and abstraction in Section. III. The proposed tree based classification algorithm and decision making process is covered in Section. IV. Classification literature associated with some existing tree based algorithms are in Section. V and finally experimental results in Section. VI.

II. MUZZLE SEGMENTATION

Given a cropped muzzle image, the first step, is to extract or estimate the muzzle contour from a noisy background which is both rich in colour as well as texture. Feature extraction can be done once this region of interest is detected and is confined to the interior of the muzzle. The role of a segmentation process is to ideally extract out the muzzle region from the background for further processing and feature extraction. Active contours using level sets are one of the most extensively used methods in image segmentation [13], [14]. This is due to their inherent ability to adapt to complex contours after a certain number of iterations, thus defining the boundary between regions in an image. The level set methods in literature are broadly categorized as edge based or region based.

In edge based level set methods, minimizing the energy functional for curve evolution is equivalent to locking the contour onto edges in an image. These methods are suitable when the object to be segmented is separated from the background by sharp edges. The distance regularization term in [15] plays a crucial role in locking the contour to complex boundaries with high edge strength. While in region based level set methods, the minimization of energy functional is equivalent to segmenting the image into homogeneous regions. The measure of homogeneity could be based on

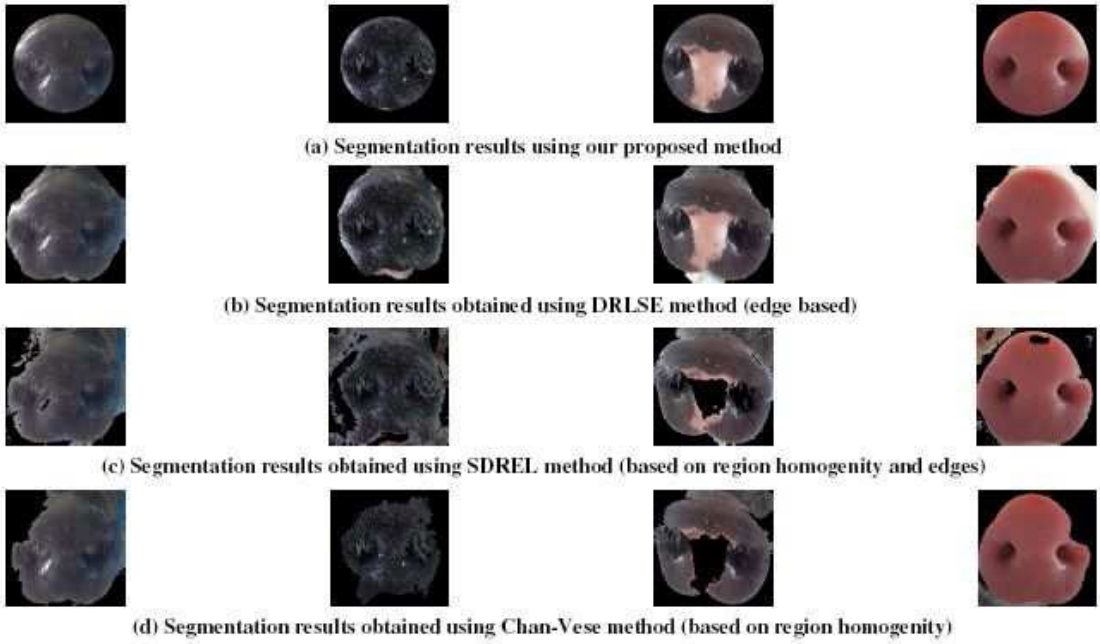

FIGURE 3. Segmented region obtained using (a)Our proposed algorithm (b)edge based DRLSE model (c)Combined region and edge based SDREL model and (d)Region based Chan-Vese model.

gray level intensity or colour or some texture-profile. In an early work by Chan *et al.* [16] involving region based level sets, a degradation in performance was observed when there was an intensity in-homogeneity either in the foreground or the background. Wang *et al.* [17], [18] later covered this issue, so long as this intensity in-homegeneity was found to be within certain bounds. Cai *et al.* [19] on the other hand used colour information guided by visual saliency for segmentation. Zhi *et al.* [20] used a combination of edge and region based methods.

However, these methods were not suitable for pig muzzle segmentation, due to the following practical on-field constraints:

- **Colour-profiling issues:** When the muzzle is snapped from the front, the region immediately around the frontal projection is usually either the face of the pig and/or partially a glove (belonging to the individual holding the pig to stabilize the head movement). Since, the colour of the face is similar to that of the muzzle surface, the background will influence the precision with which the muzzle portion can be extracted.
- **Texture-profiling issues:** From a texture viewpoint, the presence of lines, edges, corners, curves, sweat circles and hair spikes over a particular patch, impart a certain unique structure to the interior of the muzzle. Given a broad definition such as this, it becomes difficult to segregate the background containing the face of the pig (which has a rich texture due to furry and spiky hair) from the patterns on the muzzle surface.

Since standard segmentation algorithms fail, feature mixing is virtually unavoidable if one attempts an over-precise detection of the muzzle contour and its interior. Hence, instead of attempting a precise contour extraction, an attempt is made to fit in a ball inside the muzzle (with the largest possible radius), so that no part of the background is picked up. The initial goal is therefore to pre-filter the muzzle portion so that the interior gets cleaned up as much as possible and becomes largely homogeneous in appearance. While this interior is being cleaned up, the signal enhancement algorithm also enhances the contour linings without over emphasizing other parts. The segmentation algorithm must therefore achieve the following dual objective:

Selection and tuning of a suitable pre-filtering operator in a way that the muzzle contour is brought out clearly (or enhanced), while at the same time suppressing the details in the interior, making it appear partially homogeneous with respect to texture and/or colour.

Once this selective enhancement is done, a circular mask that gets nicely inscribed in the interior of the muzzle. The circular mask must be large enough to trap sufficient details both with respect to colour and texture during the feature extraction procedure. If the radius of this mask is too small (i.e. a conservative strategy to ensure the mask covers only the interior), the number of data-points available for muzzle and eventually breed characterization may become too less. On the other hand if the radius is too large this may pick up unnecessary noise associated with the background and boundary variations. Hence, the search for the optimal radius (keeping this trade-off in mind) is done over a certain band R_{MIN} and R_{MAX}. It may be noted that a part of the data in the interior of the muzzle is also lost (rather of less use), owing to the presence of two large nostrils in the muzzle interior. Hence, the minimum radius R_{MIN} must be at least large enough to go beyond the nostrils. Fig. 3 shows the muzzle

region segmented out from the background using a variety of methods such as, our proposed method; an edge based active contour model DRLSE [15]; a region based active contour model [16]; and a combination of region and edge based active contour model SDREL [20]. Active contour models which try to maintain region homogeneity by minimizing the energy functional fail miserably for cases where the muzzle region contains the pinkish white patch embedded within the grey region. These methods also fail to differentiate the facial region from the muzzle, when their colour is almost the same. The edge based methods suffer from the problem of boundary leakage, where the edges are very weak.

A. GENERATING THE CIRCULAR MASK FOR ANALYSIS

Orientation-specific Gabor filters have been used extensively to detect texture patterns in literature [9], [21], [22]. The motive for modifying and adapting these directional Gabor filters, with differentiation along one direction and smoothing along the orthogonal direction, was to enhance the step edges, trapping parts of the main contour. The smooth regions are expected to register a lower detection-score as compared to the edges. In this case to enhance the relatively sharp muzzle contour as compared to the smooth interior a quantized Derivative of a Gaussian (DGau) function is presented in its discretized form as: $D(x) = -xe^{-x^2/(2\sigma_f^2)}$. Here, σ_f is the standard deviation associated with this Gaussian and $x \in \{-L, .., 0, \ldots, L\}$, with $L = \lfloor 3\sigma_f \rfloor$ (with $\lfloor\rfloor$ representing the floor function). The base kernel is created by rotating the discretized version in the X-Y plane. The kernel has two degrees of freedom: (i) Standard deviation σ_f associated with the differentiation process along a certain line and (ii) thickness t associated with a smoothing along a direction orthogonal to the orientation of the DGau function. If $\delta_{1D}(m)$ represents the 1D Kronecker delta function and $\delta_{2D}(m, n)$ represents the 2D Kronecker delta function defined as follows:

$$\delta_{1D}(m) = 1 \text{ IF } m = 0 \text{ and '0' if } m \neq 0 \quad (1)$$

$$\delta_{2D}(m, n) = 1 \text{ IF } (m = 0, n = 0) \text{ and '0' if } (m \neq 0 \text{ or } n \neq 0) \quad (2)$$

Both $(m, n) \in Z$, the set of integers. The 2D linear convolution denoted by the operator $'*'$ between two functions $g_1(x, y)$ and $g_2(x, y)$ is defined as:

$$f(x, y) = g_1(x, y) * g_2(x, y) = \sum_{u=-\infty}^{\infty} \sum_{v=-\infty}^{\infty} g_1(u, v) g_2(x - u, y - v) \quad (3)$$

Each arm of the $'*'$ operator has two wings: one a derivative filter and the other a smoothing filter in the orthogonal direction. The Gaussian derivative filter function is given by,

$$h_1(x, y) = D(x); \text{ for } y = 0 \quad (4)$$

Written compactly as,

$$h_1(x, y) = \sum_{u=-\infty}^{\infty} D(u)\delta_{2D}(x - u, y) \quad (5)$$

The smoothing wing is given by:

$$h_2(x, y) = \sum_{u=-\frac{(t-1)}{2}}^{\frac{(t-1)}{2}} \delta_{2D}(x, y - u) \quad (6)$$

$$h_{c,0F}(x, y, \theta = 0^0) = h_{BASE}(x, y) = h_1(x, y) \star h_2(x, y) \quad (7)$$

This is equivalent to running the first filter h_1 over the entire image and following it up with h_2 (or vice-versa). The first filter which is the DGau filter, eliminates zones where the intensity profile is largely homogeneous and converts step edges to thick lines. The second filter, depending on the thickness parameter t, serves as a brush (whose thickness is decided by t) in extending the impact of the directional gradient over a small neighborhood. Due to this all homogeneous patches of size $t \times 2L$ are nullified. Here, this texture homogeneity refers to a set of horizontal stripes.

$$h_{c,120}(x, y, \theta = 120^0) = \textit{Rotation of base function by } 120^0 \textit{ counter} - \textit{clockwise} \quad (8)$$

Let (X, Y) be the new coordinates when the reference system is rotated in the counter-clockwise direction by an angle θ and let (x, y) the coordinates with respect to the original reference system.

$$x = X\cos(\theta) - Y\sin(\theta)$$
$$y = -X\sin(\theta) + Y\cos(\theta) \quad (9)$$

And in this new reference frame,

$$h_{c,120}(x = X\cos(\theta) - Y\sin(\theta), y = -X\sin(\theta) + Y\cos(\theta)) = h_{BASE}(X, Y) \textit{ with } \theta = 120^0 \quad (10)$$

A similar pattern is followed for the other function positioned at 240 degrees. The generated plots are shown in Fig. 4. There are in fact three primary, directional Gabor-type filters in operation, whose results are fused for different parameter values: $\sigma_f \in 1, 3, 5, 9$ and $t \in 1, 3, 5, 11$ using the square energy linked relation [9]. The final texture profile is,

$$I_F(x, y, \theta) = IM(x, y) \star h_{c[\theta]F}(x, y)$$
$$T(x, y) = I_F(x, y, 0^0)^2 + I_F(x, y, 120^0)^2 + I_F(x, y, 240^0)^2 \quad (11)$$

When the orientation of this kernel is changed along the X-Y plane to 120^0 and 240^0 (Fig. 4), this definition of homogeneity extends to include elimination of lines at other orientations. Curves can also be eliminated provided the curvatures at points where there is a change in direction is not significant. Pores are also eliminated.

The global mean is computed as

$$\mu_{GL} = \frac{1}{N^2} \sum_{x=1}^{N} \sum_{y=1}^{N} T(x, y) \quad (12)$$

and the final quantized binary representation is given by,

$$BIN_{TEX}(x, y) = 1 \text{ IF } T(x, y) > \mu_{GL} \text{ and '0' otherwise} \quad (13)$$

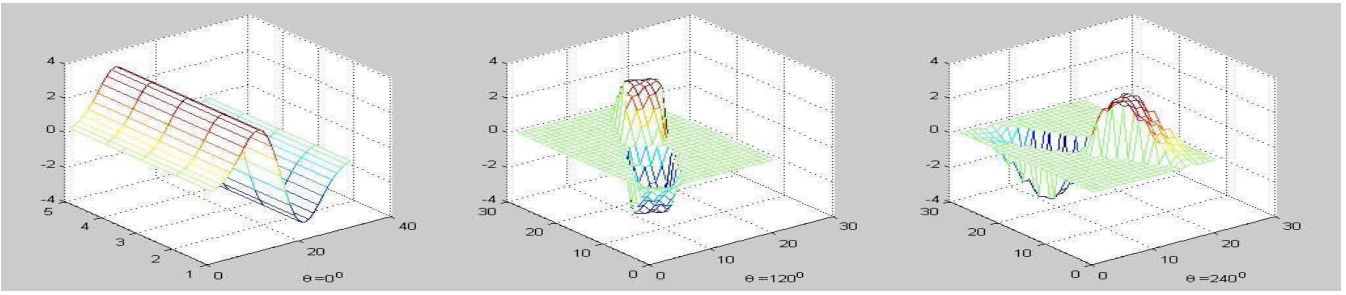

FIGURE 4. Structure of the directional (orientation specific) DGau filters corresponding to three different angles: 0^0, 120^0 and 240^0, all with respect to the X-axis.

for $x, y \in 1, 2, ..N$ ($N = 512$). An increase in σ_f tends to thicken the contour profiles as the DGau function tends to operate along the normal to the contours. To apply this design, it is recognized that the muzzle pre-filtering procedure has two degrees of freedom: (i) **Standard deviation,** σ_f The strength of the orientation specific DGau-differentiator can be adjusted by increasing or decreasing σ_f. Because of the circular symmetry of triad-arrangement (0^0, 120^0, 240^0), most line artifacts owing to the presence of hair in the muzzle interior can be eliminated. This triad-arrangement is fixed. The interior of the muzzle has many sweat pores (in some cases covered by stunted hair), which emerge as spikes. These spikes can be suppressed if the value of σ_f is sufficiently large (illustrated in Fig. 6 with respect to the muzzle of the Ghungroo pig in Fig. 5). When this DGau is aligned with a line artefact, the line can be removed completely. But since the hair on the muzzle may have arbitrary orientations, this line elimination is indirectly facilitated through a projection mechanism involving three DGau along three different directions (indicated by the filters in Fig. 4); (ii) **Thickness,** t The effectiveness of the brush work involved in cleaning up the interior increases with t. This also increases the tolerance of the triad-DGau structure to multiple line thicknesses, sweat pores of different sizes and arbitrary short curves. But too large a thickness t has a tendency to enhance step edges particularly in the case of breeds which have pink-patches in the interior, such as Hampshire and Duroc. Furthermore, this increase in t may lead to an overemphasis of the contours associated with the pig's nostrils (which is unnecessary).

To crystallize the parameters calibration is done with respect the most noisy breed, which happens to be Ghungroo and then test the final set on all. To identify the right choice of parameters, σ_f is varied over the set $\{1, 3, 5, 9\}$ and the thickness is varied from $1, 3, 5, 7$. The original cropped Ghungroo muzzle image is shown in Fig. 5 in which the impact of the Gabor filtering followed by the binarization procedure is witnessed. High texture homogeneity within the Ghungroo-muzzle contour is obtained for $\sigma_f = 4; t \geq 3$, as indicated in the sub-figures inside the red-rectangle in Fig. 6.

FIGURE 5. Muzzle of Ghungroo pig for DGau pre-filtering and texture quantization.

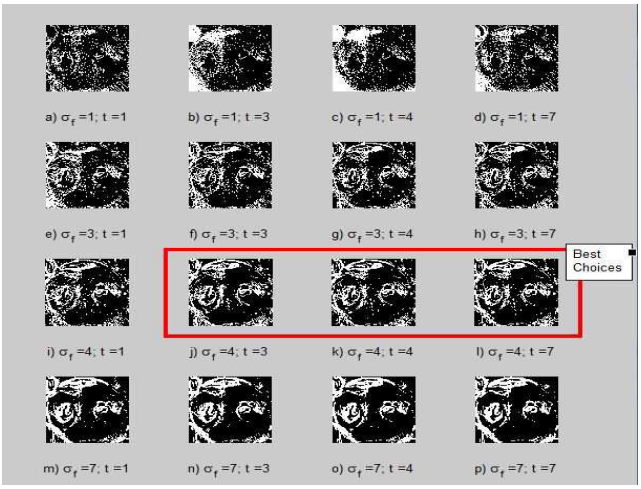

FIGURE 6. Impact of DGau pre-filtering and texture quantization on the muzzle of a Ghungroo pig (Fig. 5).

Once the binary segmentation map $BIN_{TEX}(\sigma_f, t)$ is created for the best choice of parameters $\sigma_f = 4$ and $t = 3$, two thresholds R_{MIN} and R_{MAX} are to be set and for all (x, y), such that, $BIN_{TEX}(x, y) = 1$ AND $\sqrt{(x - x_c)^2 + (y - y_c)^2} > R_{MIN}$ (whose distance is larger than R_{MIN}), the distance from the center of the map (x_c, y_c) is computed as, $D_s = D_{SEL}(x_s, y_s) = \sqrt{(x_s - x_c)^2 + (y_s - y_c)^2}$. Here, (x_s, y_s), $s \in 1, 2, .., N_s$ are the significant points indicated by the binary map which have a distance larger than R_{MIN} and lesser than R_{MAX}. From this set, the mask radius is estimated as the median over the entire set.

$$R_{MASK} = MEDIAN(D_s), s \in \{1, 2, 3, \ldots N_s\} \quad (14)$$

TABLE 2. Table showing the mean classification accuracies along with the standard deviation across 100 iterations with different train and test data for the four breeds viz. DUROC(D), GHUNGROO(G), HAMPSHIRE(H) and YORKSHIRE(Y) as a function of R_{MIN} and R_{MAX}.

	$R_{MIN}=0.6$ $R_{MAX}=0.7$	$R_{MIN}=0.6$ $R_{MAX}=0.8$	$R_{MIN}=0.6$ $R_{MAX}=0.9$	$R_{MIN}=0.6$ $R_{MAX}=0.95$	$R_{MIN}=0$ $R_{MAX}=0.7$	$R_{MIN}=0$ $R_{MAX}=0.8$	$R_{MIN}=0$ $R_{MAX}=0.9$	$R_{MIN}=0$ $R_{MAX}=0.95$
μ_D	63.16	70.13	84.74	85.82	60.71	67.31	72.67	76.15
σ_D	10.63	20.25	14.53	12.68	20.23	19.42	22.37	17.26
μ_G	88.55	90.56	96.88	93.80	83.51	85.23	90.19	91.74
σ_G	6.18	9.61	5.69	7.90	12.72	9.84	7.13	7.58
μ_H	76.53	79.64	85.18	86.62	69.81	71.22	76.45	82.39
σ_H	9.90	10.33	12.74	12.84	11.22	13.15	9.89	8.19
μ_Y	98.16	96.86	98.92	98.24	94.91	96.95	98.71	98.13
σ_Y	2.11	3.80	1.19	2.15	4.98	4.83	2.35	2.86

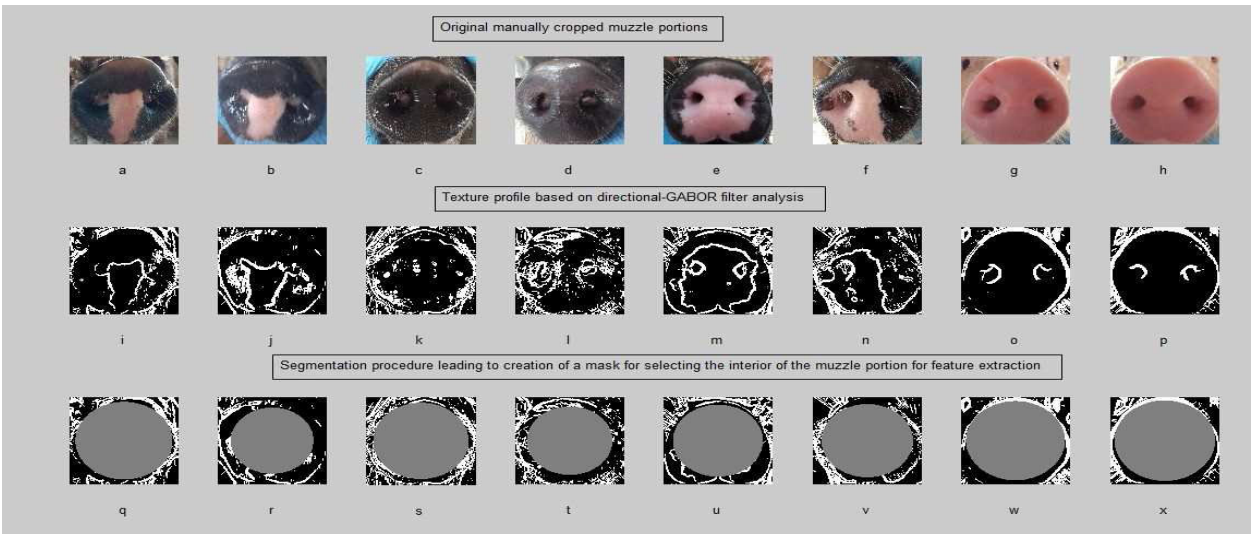

FIGURE 7. Results of adaptive circular mask generation process for pigs from different breeds.

Thus R_{MASK} is obtained in an adaptive manner and it is not fixed for all the muzzle images. It is dependent upon the nature of the contour which is picked up by the DGau operator, the noise inside the muzzle contour picked up and also the region of computation as defined by R_{MIN} and R_{MAX}. The choice of R_{MIN} should be such that the nostrils on the muzzle surface can be avoided from the computation of R_{MASK}. This is because these nostrils act as a deterrent in the computation of R_{MASK} as their edges tend to produce a false response to the DGau operator. R_{MAX} should be chosen in such a way so as to avoid the background region from affecting the computation of R_{MASK} on an image adaptive basis (i.e. for every new muzzle image this parameter is re-computed). The impact of R_{MIN} and R_{MAX} on the classification accuracies are tabulated in Table 2, when this image-adaptive ball of radius, R_{MASK}, with $R_{MAX} < R_{MASK} < R_{MAX}$ is placed inside muzzle with the help of the Gabor-triad filter arrangement. From this table it can be easily observed that the best classification accuracies are obtained for $R_{MIN} = 0.6 \times (N/2)$ and $R_{MAX} = 0.95 \times (N/2)$. The necessity of this adaptive mask generation algorithm can also be easily understood from the classification accuracies in Table 3, where a fixed value of R_{MASK} has been used for all the muzzle images. The accuracies drop significantly in this case, for all the values of $R_{MASK} = R_{FIXED}$, mentioned in Table 3.

TABLE 3. Table showing the mean classification accuracies along with the standard deviation across 100 iterations with different train and test data for the four breeds viz. DUROC(D), GHUNGROO(G), HAMPSHIRE(H) and YORKSHIRE(Y) with fixed value of R_{MASK}.

	$R_{MASK}=0.7$	$R_{MASK}=0.8$	$R_{MASK}=0.9$	$R_{MASK}=0.95$
μ_D	59.93	65.96	75.75	75.21
σ_D	20.97	19.71	20.63	13.76
μ_G	87.53	89.95	90.80	89.85
σ_G	9.47	12.55	10.40	10.57
μ_H	73.48	75.74	81.97	79.17
σ_H	8.42	7.35	10.31	11.62
μ_Y	98.98	98.53	98.40	97.39
σ_Y	1.67	2.57	3.52	3.18

Results of this adaptive circular mask generation process are shown in Fig. 7.

III. SELECTING AND GENERATING VISUAL DESCRIPTORS FOR THE MUZZLE REGION

Once the segmented region is extracted from the interior of the muzzle, this region of interest can now be analyzed on two fronts: Colour and Texture. Depending on the positioning of the light source and the manner in which the pig's snout is being held, there will be significant illumination

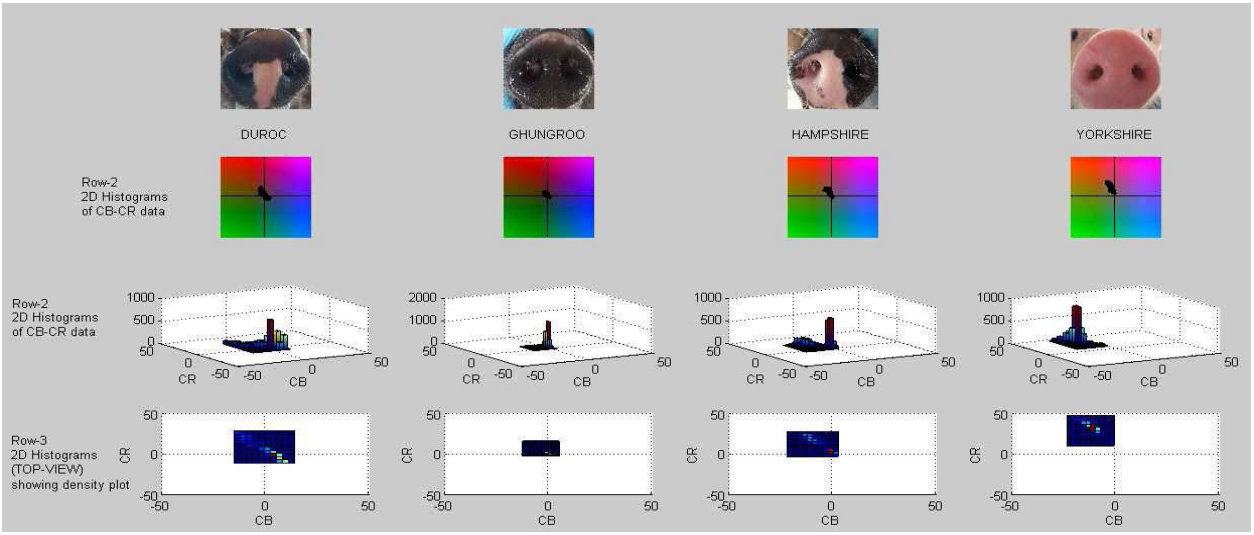

FIGURE 8. Scatter plots and 2D histograms in the Cb-Cr domain (four pig breeds).

variations across pigs from the same breed. This results in considerable intra-class variability. To ensure a robust colourimetric analysis, the luminance segment must be segregated from the chrominance part and thus the image must be first be converted from RGB space to another apprpriate colour space. The luminance component gets decoupled from the chromatic part when the image is analyzed in the YCbCr space, making the Chromatic components (C_b and C_r) independent of the local illumination profile and variations as shown in [23]. Some muzzle samples from the four breeds (corresponding to $4 \times 2 = 8$ different pigs: two per breed), are shown in Fig.7, with the photographs taken under natural lighting conditions (viz. in a shed in broad daylight). Here initially, the procedure for qualifying the proposed colour descriptor based on a 2-dimensional histogram over the chrominance space (or Cb-Cr-space), is discussed. In the next part, the procedure for arriving at the right choice of parameters based on two texture descriptors (one the GSM [2] and the other the top-hat morphological operator [24], which can be used for extracting bright spots from dark background [25]), is presented.

A. SELECTION OF THE COLOUR DESCRIPTOR

It was summarized in Table. 1, that the colour composition of the muzzle surface was distinct for these four breeds: Duroc, Ghungroo, Hampshire and Yorkshire. Examples indicating both intra-class variability as well as breed separability with respect to colour (Fig. 2(a-d) and Fig. 7(a-h)). In some cases, the muzzle of Duroc carries a pinkish-white patch (whose size and position is un-predictable). Hampshire male pigs on the other hand show a strong and consistent pink-patch presence (again the size and position of the patch is variable, but generally found much larger than the ones found in the odd Duroc pig). Yorkshire pig-muzzles are completely pink in colour, which makes them easily identifiable and separable from pure-greyish black Ghungroo pigs. The main confusion thus arises between Duroc and Hampshire both with respect to colour and texture. In the colourimetric part of the $Y - C_b - C_r$ space, this separation can be tapped statistically via 2-dimensional histograms (Fig. 8 (third and fourth rows)). It is evident from row-4 (top-view of the $C_b - C_r$ histograms), that the chromatic-centroids of Duroc, Ghungroo, Hampshire and Yorkshire are all distinct (Fig. 8, fourth row). The footprints of the histograms in the (a-b) space are much larger for Duroc, Hampshire and Yorkshire as compared to Ghungroo. The colour diversity is much less in the case of Ghungroo and maximum for Duroc (Fig. 8, fourth row). Thus, the histogram features are distinct for all the four breeds, which qualifies this primary feature as a robust yet distinctive colour descriptor for breed-segregation.

Colour measurements were taken over the muzzle surface for a particular pig (only confined to the mask region), through a random sampling procedure. After picking random samples of the pixels within the mask region, the following dataset was generated, associated with chroma measurements ($C_b - C_r$ space):$CDATA_{PIG,BR} = \{(u_1, v_1), (u_2, v_2), \ldots .(u_n, v_n)\}$, with n being the number of data-points picked randomly inside the muzzle. The muzzle images were resized to 512×512 and all points within the circular mask were considered for the 2D histogram generation and colourimetric analysis. Robust statistics from this histogram such as, marginal and joint moments, secondary statistics such as Sarle's bimodality coefficient [10], both at a 1-D level and also at a 2-D level with the assumption of independence were computed. All the moments were normalized with respect to the standard deviations in both the dimensions (C_b, C_r). Let $f_H(\tilde{u}, \tilde{v})$ denote the 2-dimensional normalized histogram associated with the chromatic-components (C_b, C_r) linked to the muzzle-colour profile of a particular pig belonging to a certain breed $BR \in 1, 2, 3, 4$. This in essence is a 4-class classification problem where class-1 corresponds to the Duroc breed of pigs,

class-2 to Ghungroo, class-3 to Hampshire and class-4 to Yorkshire. here the variables $\tilde{u}$ and $\tilde{v}$ takes the C_b and C_r values respectively of a particular pixel. The ordered pair $(\tilde{u}, \tilde{v}) \in Z \times Z_S$, where $Z_S = [-128, -127, \ldots, 128]$. If $(u_i, v_i), i = 1, 2, \ldots, n$ denote the (C_b, C_r) values of the n randomly selected pixels in the region defined by the circular mask, then $f_H(\tilde{u}, \tilde{v})$ is defined as

$$f_H(\tilde{u}, \tilde{v}) = \sum_{i=1}^{n} \delta_{2D}(\tilde{u} - u_i, \tilde{v} - v_i) \tag{15}$$

Since $f_H(\tilde{u}, \tilde{v})$ is a 2-dimensional histogram, hence it has the following properties:

$$0 \leq \left(\frac{1}{n}\right) f_H(\tilde{u}, \tilde{v}) \leq 1$$
$$\left(\frac{1}{n}\right) \sum_{\tilde{u}=-128}^{128} \sum_{\tilde{v}=-128}^{128} f_H(\tilde{u}, \tilde{v}) = 1 \tag{16}$$

The statistics computed on this sub-sampled dataset tend to characterize the histograms seen in Fig. 8. Of interest are the following parameters: (P1) Bi-modality Index [10]: In breeds like Hampshire and Duroc, muzzles tend to show a pink patch and the rest of the muzzle is either greyish-black or powdery-black. Thus the histograms in these two cases (if a pink patch is indeed present in the Duroc pig), tend to be of a bi-modal nature. This bi-modality, reflects as a heavy-tailed distribution and hence as per the literature [10] can be trapped using a combination of the Skewness and Kurtosis. Extension to 2-dimensional data is done here based on certain assumptions; (P2) Centroid: Mean vector associated with the pair Chroma-pair (C_b, C_r) (black for Ghungroo, weighted combination of black and pink for Hampshire, pink for Yorkshire and selective weighting (black,pink) for Duroc; The centroids are definitely expected to be distinct for Ghungroo, Yorkshire and Hampshire; (P3) Footprint of the distribution: This is obtained through a principal component analysis (PCA), over the chroma-space, by first overlooking the bi-modal possibility and assuming it to be of a unimodal 2-dimensional Gaussian type. The square-root of the product of the eigenvalues is expected to provide and estimate of the footprint of the distribution; (P4) Skewness and Kurtosis of both the C_b and C_r data (to be used for computing the composite bi-modal index assuming independence of the colour-channels). The corresponding equations for parameters P1, P2, P3 and P4 are constructed in the following way: First the means of the respective chromatic components C_b and C_r are computed to generated the centroid: $\mu_{C_b} = \frac{1}{n}\sum_{i=1}^{n} u_i$ and $\mu_{C_r} = \frac{1}{n}\sum_{i=1}^{n} v_i$. Then the Kurtosis and Skewness measures for the respective chromatic components C_b and C_r were computed as,

$$SKEW_{C_b} = \frac{\frac{1}{n}\sum_{i=1}^{n}(u_i - \mu_{C_b})^3}{(\sqrt{\frac{1}{n}\sum_{i=1}^{n}(u_i - \mu_{C_b})^2})^3}$$
$$KURT_{C_b} = \frac{\frac{1}{n}\sum_{i=1}^{n}(u_i - \mu_{C_b})^4}{(\frac{1}{n}\sum_{i=1}^{n}(u_i - \mu_{C_b})^2)^2} \tag{17}$$

In a similar fashion $SKEW_{C_r}$ and $KURT_{C_r}$ are computed. Based on Sarle's proposition [26], bi-modality can be predicted using the heavy tailed nature of the respective chroma marginal probability distributions, which in turn reflects in the higher order moments: Skewness and Kurtosis. This Bi-modality index can be computed for the respective chromatic components C_b and C_r as,

$$BIM_{C_b} = \frac{1 + SKEW_{C_b}^2}{KURT_{C_b}} \tag{18}$$

with a similar form for the C_r-component, BIM_{C_r}. Assuming independence of the chromatic components C_b and C_r, a 2D bi-modality coefficient approximation can be generated as a geometric mean of the bi-modality coefficients of C_b and C_r,

$$BIM_{APP(2D)} = \sqrt{BIM_{C_b} \times BIM_{C_r}} \tag{19}$$

To establish the size of the footprint of the joint $C_b - C_r$ probability distribution, a PCA analysis is done to compute the eigenvalues λ_1 and λ_2. The eigenvectors are discarded as they are expected to be data-sensitive but the eigenvalues are retained. Let the data-vector be $\bar{v}_i = [u_i, v_i]^T$ and the centroid $\bar{v}_{CEN} = [\mu_{C_b}, \mu_{C_r}]^T$. First the colour covariance matrix over the $C_b - C_r$ space is computed as:

$$S_{C_bC_r} = \frac{1}{n}\sum_{i=1}^{n}(\bar{v}_i - \bar{v}_{CEN})(\bar{v}_i - \bar{v}_{CEN})^T \tag{20}$$

Let the eigen-decomposition of this matrix be,

$$S_{C_bC_r} = VDV^H \tag{21}$$

where, D is a diagonal eigenvalue matrix comprising of two eigenvalues: λ_1 and λ_2. The footprint of the joint probability distribution can be approximated as,

$$FOOT_{C_bC_r} = \sqrt{\lambda_1 \times \lambda_2} \tag{22}$$

The skew associated with this footprint, about the eigen-directions can be quantified as,

$$FOOT_{SKEW} = \frac{MIN(\lambda_1, \lambda_2)}{MAX(\lambda_1, \lambda_2)} \tag{23}$$

The final colour descriptor or feature vector is given by this seven-dimensional vector (collection of selective statistics/ descriptors computed over the $C_b - C_r$ muzzle-data within the mask region): $\bar{f}_{COLOR} = [cd_1, cd_2, cd_3, cd_4, cd_5, cd_6, cd_7]^T$. Here, $cd_1 = \mu_{C_b}$, $cd_2 = \mu_{C_r}$, $cd_3 = BIM_{C_b}$, $cd_4 = BIM_{C_r}$, $cd_5 = BIM_{APP(2D)}$, $cd_6 = FOOT_{C_bC_r}$, and $cd_7 = FOOT_{SKEW}$. The t-SNE map [27], which is indication of the extent of feature separability across these four breeds is shown in Fig. 9.

B. TEXTURE DESCRIPTORS

The muzzle of each pig shows significant structural details which can be detected by suitable operators or filters. The following are some observations regarding this structural arrangement:

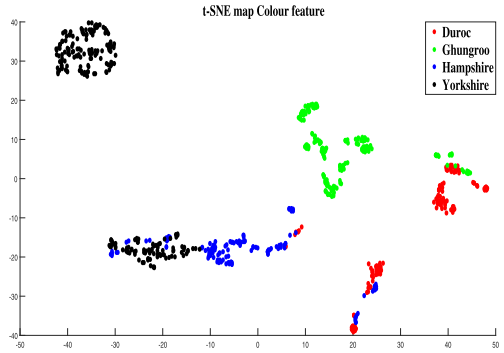

FIGURE 9. 2-dimensional t-SNE map for colour.

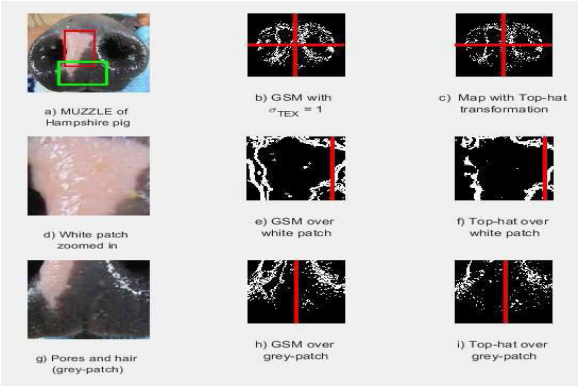

FIGURE 10. Patch related texture variations seen in a Hampshire pig.

- Sweat pores are present all over the muzzle surface both on the pinkish-white regions (present in breeds such as Hampshire, Duroc and all-pink Yorkshire), as well as the greyish-black patches (present in breeds such as blackish-Ghungroo, dual-coloured Hampshire and selectively dual-coloured Duroc).
- Hair or cilia (both prominent as well as stunted) are different for different breeds. Firstly these are confined to the greyish-black regions and do not exist over the pink patches. Over the greyish-black patches this density is more or less uniform and high. Hence, Ghungroo, which is all black, exhibits a high density of pores and hair (both stunted and long) all around the dial, while in the case of Yorkshire, there are no hair/stunted hair on the muzzle surface.

The objective of any texture filter should be to produce distinct and different results/outputs for different breeds, while swallowing the variability within the same class. The texture details present on the muzzle surface need to be highlighted out at their corresponding location on the muzzle surface for this purpose. There are several texture descriptors available in literature [28]. Two texture filters/descriptors have been used for trapping the significant portions in the muzzle region where there are structured artifacts related to sweat-pores, hair, stunted hair, patch transition regions (or contours) and in some cases wrinkles in the skin. The Gradient Significance Map(GSM) [2] and the Top-hat (THAT) morphological transformation [24] are used to generate significance maps which can then be quantized to produce what are known as patch density maps(PDMs) [2]. If $BM(x, y) : x, y \in \{1, 2, \ldots, N\}$ is a binary significance map (either of GSM or THAT type), this map is split into four quadrants and the fraction of white/significant pixels are counted and recorded in each quadrant. Fig. 10(a) shows the muzzle of a Hampshire pig and Fig. 10(b,c) shows the differential information obtained from the significance maps with respect to GSM and THAT along with the quadrant PDM scores. The contour present in the interior, because of the pink patch in the Hampshire pig, is picked up by the GSM but not by the THAT-operator. This distinction becomes useful while segregating Hampshire and Yorkshire with respect to texture.

The significance map associated with GSM is a function of the Gaussian gradient parameter, i.e. the standard deviation parameter (σ_{TEX}), while the top-hat morphological operator is primarily a function of the radius of the structuring element r. It has been observed [2] that a small value of σ_{TEX} tends to enhance the noise leaking into the feature calculation, while a large value suppresses key internal details on the muzzle's surface. For the morphological THAT operator, the dimension of the structuring element must be carefully selected [24]. The main objective of using this operator is to enhance fine details like the hair follicles and pores on the muzzle surface, while filtering out the coarse details. Hence, a structuring element with a small dimension is desirable. The corresponding quadrant-wise density feature vectors, related to the GSM and TOP-HAT maps are given by,

$$\begin{aligned} D_{GSM}(\sigma_{TEX}) &= [p_1, p_2, p_3, p_4]^T \\ D_{THAT}(r) &= [q_1, q_2, q_3, q_4]^T \end{aligned} \tag{24}$$

where, $p_i, q_i \in [0, 1]$ and $i \in \{1, 2, 3, 4\}$. In the case of the Hampshire pig, owing to the presence of the pink-patch, there is a prominent internal contour which is picked up by the GSM but slightly suppressed in the TOP-HAT map. Thus the texture filter outputs (GSM vs TOP-HAT) are different for Hampshire (Fig. 11). The lack of details within the pinkish-white patch in the Hampshire pig is demonstrated in Fig. 10(d,e,f). Much of the details (dot, blob, line and curve artifacts) are concentrated over the greyish-black zone, Fig. 10(g,h,i). To account for the overall density scores over the four quadrants for Ghungroo (most cases found to be high) and lowest for Yorkshire, two mean parameters have been derived from the GSM and TOP-HAT quadrant

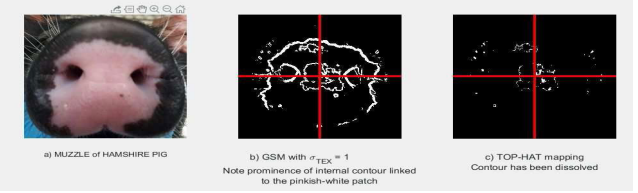

FIGURE 11. Texture profile and patch density scores for a Hampshire pig.

density scores.

$$\mu_{GSM} = \frac{p_1 + p_2 + p_3 + p_4}{4}$$
$$\mu_{THAT} = \frac{q_1 + q_2 + q_3 + q_4}{4} \quad (25)$$

The final texture feature vector is a 10-dimensional vector, a function of two primary parameters: σ_{TEX} from the GSM and structural elemental radius r for the top-hat operator.

$$\bar{f}_{TEX}(\sigma_{TEX}, r) = [p_1, p_2, p_3, p_4, q_1, q_2, q_3, q_4, \mu_{GSM}, \mu_{THAT}]^T \quad (26)$$

To verify the robustness and distinctiveness characteristic of this feature vector, muzzle images of 20 pigs (five per breed), were chosen for the experiment. The four breeds were Duroc, Ghungroo, Hampshire and Yorkshire. The Gaussian gradient parameter σ_{TEX} was varied over the range of $\sigma_{TEX} \in \{2, 4, 6, 8, 10\}$ and the radius of the top-hat structuring element was varied as $r \in \{2, 3, 5, 7, 9\}$.

In order to assess the performance of the texture feature as a function of the smoothing parameter from the GSM (σ_{TEX}) and radius (r) of the structuring element from the THAT-operator, the overall separability across breeds for different parameter settings was computed. This was done using a metric based on the Mahalanobis distance [29] for measuring cluster/class separability. Five muzzle images selected from five different pigs per breed were chosen for this purpose; leading to four different sets of feature vectors. Let BR_1,BR_2, BR_3 and BR_4 represent the four breeds/clusters. Then $d_{MD(i)}(j)$ is chosen to be the Mahalanobis distance from the centroid of the cluster BR_i to cluster BR_j. First, the distance of breed BR_1 from each of BR_2, BR_3 and BR_4 is measured individually. The overall distance of BR_1 (denoted by $\bar{d}_{MD(1)}$) from the other three classes is the mean of the individual distances of BR_1 from the other three classes, i.e.,

$$\bar{d}_{MD(1)} = (d_{MD(1)}(2) + d_{MD(1)}(3) + d_{MD(1)}(4))/3 \quad (27)$$

In a similar manner, distances $\bar{d}_{MD(2)}$, $\bar{d}_{MD(3)}$ and $\bar{d}_{MD(4)}$ are measured. The overall separation between the four breed datasets is the mean over those four scores.

$$SM(\sigma_{TEX}, r) = \frac{\bar{d}_{MD(1)} + \bar{d}_{MD(2)} + \bar{d}_{MD(3)} + \bar{d}_{MD(4)}}{4} \quad (28)$$

From the separation scores produced in Table. 4, $\sigma_{TEX} = 4$ and $r = 3$ are obtained as the best parameter set for extraction of robust texture features. The corresponding t-SNE [27] map which brings out the feature separability across breeds for the optimal parameter set $\sigma_{TEX} = 4$ and $r = 3$ from Table. 4 is shown in Fig. 12.

IV. TREE SYNTHESIS PROCEDURE

As observed from the t-SNE maps in Section III, feature vectors obtained from the colour or texture information alone are not self-sufficient for breed discrimination. Simply combining the texture and colour features into one single composite vector may help, but may prove to be sub-optimal in cases where on a breed-specific basis, there is a correlation between the colour and texture features/maps in some breeds, while there is a disassociation in others. This inconsistency, renders classification based on a singular mixed feature, fixed decision space less effective. This calls for a hierarchical selection procedure. This is the motivation for taking a graph-theoretic approach mainly for identifying the order and manner in which the breeds are siphoned out in the proposed classification procedure. A decision tree is constructed whose leaves form the breed-nodes but the difference here is that unlike a conventional decision tree algorithm which does random attribute sampling and model building and adaptation to arrive at the optimal decision space at each node, the feature selection in our proposed tree building algorithm is done at the MACRO level and NOT at the attribute level.

TABLE 4. Separation scores for the composite texture feature for different values of σ_{TEX} (GSM-operator) and different radii r (THAT [24] morphological operator).

	$r=2$	$r=3$	$r=5$	$r=7$	$r=9$
$\sigma_{TEX}=2$	31.50	45.04	39.33	35.57	35.77
$\sigma_{TEX}=4$	43.77	**52.41**	41.41	35.94	35.65
$\sigma_{TEX}=6$	44.30	51.77	41.18	35.43	36.68
$\sigma_{TEX}=8$	41.33	49.59	40.47	34.80	37.08
$\sigma_{TEX}=10$	36.73	46.37	37.92	32.27	34.78

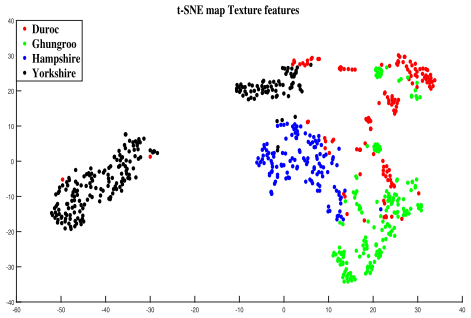

FIGURE 12. t-SNE map of the texture feature set.

A. CLUSTER/CLASS SEPARATION INDICATORS

The distance metric between any two classes should properly portray the separability between these two classes assuming that this frame is modeled using a binary linear classifier (two class separation problem). First a linear discriminant classifier is learnt from the data taken from the two classes which attempts to separate the two classes with minimum error. There are two independent indicators for this cluster separation:

1) FRACTIONAL CROSSOVERS

Here,the number of crossovers on either side of the hyperplane is used as a measure of separability. More the fractional number of crossovers, lower is the separability between the two classes (and greater is the class mixing). Let n_i and n_j denote the number of members in class i and class j respectively and n_{ij} the number actually belonging to class i but falling on the other side of the hyperplane. This distance

TABLE 5. Histogram type for colour and conditional distribution for texture density along with the correlation between (C) and (T) feature sets for various breeds.

Breed type	Histogram type for Color	Conditional distribution for Texture density	Correlation between Color and Texture feature parameters
Duroc	Color histogram can be either bi-modal or uni-modal(if uni-modal the spread is narrow).	Moderate to low texture density and moderate variability.	Virtually independent.
Ghungroo	Limited variability as far as color (grey shades) are concerned.	High density in texture but variability on the higher side.	Weak correlation (virtual independence of color and texture features).
Hampshire	Bi-modal.	Bi-modal.	Moderate to strong.
Yorkshire	Moderate variability in pink shades.	Low density in texture and limited variability (non-existent in most Yorkshire pigs).	Strong correlation

indicator is,

$$SEP_{CO}(i,j) = 0.5 \times \left(2 - \frac{n_{ij}}{n_i} - \frac{n_{ji}}{n_j}\right) \tag{29}$$

A value of $SEP_{CO}(i,j) \approx 1$ indicates that the classes are clearly separable (via a linear classifier).

2) NORMALIZED CLUSTER DISTANCE

Here the separation between the clusters is of greater concern as compared to the overlap between them. Non-overlapping closely positioned clusters are penalized as compared to more separated ones. A hyperplane is first learnt for separating the two classes using a linear discriminant classifier. A certain fraction of data is chosen from each of the two classes, which are nearest to the learnt hyperplane. Note that all of these chosen data points from either of the classes are the ones which fall on the respective side of the hyperplane to which they actually belong to. Let $\mu_{D(i)}(\alpha)$ and $\mu_{D(j)}(\alpha)$ denote the mean distance of these α-fraction of the nearest data-points of class i and class j respectively from the hyperplane. Then, distance metric along the second dimension is defined as

$$SEP_D(i,j) = \left(\frac{S(\alpha)}{1+S(\alpha)}\right)$$
$$S(\alpha) = \frac{\mu_{D(i)}(\alpha)}{\sigma_{D(i)}(\alpha)} + \frac{\mu_{D(j)}(\alpha)}{\sigma_{D(j)}(\alpha)} \tag{30}$$

The role of standard deviation based normalization as far as the Euclidean distances are concerned is to penalize clusters which are non-compact (same centroidal separation, but show greater variability). The separation indicator is,

$$SEP_{OVERALL}(i,j) = SEP_{CO}(i,j) + SEP_D(i,j) \tag{31}$$

over range [0,2]. Table 6 gives the mean separation between two different breeds as a function of the feature/composite feature used over 100 different random selections of training data as will be explained later in Section. VI. It can be observed from Table 6 that out of the six breed-pairs, there are instances when either the color (C) or texture feature (T) alone gives better class separability as compared to the union of colour and texture features ($C \cup T$). Thus in the union of colour and texture features, the union may take place

TABLE 6. Distance metric for all possible binary splits when two breeds are present: D:Duroc, G:Ghungroo, H:Hampshire, Y:Yorkshire; C: Colour features, T: Texture features, $T \cup C$: Composite features; Largest distances in each column are indicated in BOLD font.

	D-G	D-H	D-Y	G-H	G-Y	H-Y
C: Colour	**1.90**	1.71	1.74	**1.94**	**1.97**	1.64
T: Texture	1.67	**1.83**	1.81	1.81	1.95	1.87
$C \cup T$	1.71	1.74	**1.93**	1.87	1.94	**1.87**
Best features	C	T	$C \cup T$	C	C	$C \cup T$
MAX-distances	1.90	1.83	1.93	1.94	1.97	1.87

constructively or destructively, so that the class separation either increases or decreases respectively. Upon examining a combination of feature sets such as (C) and (T), the correlation profiles between these two feature sets in different breeds are expected to be different. Thus there is expected to be a mismatch between the correlation trends which affects the cluster separation in this common decision space ($C \cup T$). There is therefore a need to exercise a judgement as to whether both features have to be included and if not, which one is the preferred choice to form the decision space. The correlation profiles between the feature sets (C) and (T) in different breeds are expected to be different which is listed in Table 5.

Since the correlation between the feature sets (C) and (T) is strong both for Hampshire and Yorkshire, hence the distance metric is observed to be maximum for the feature set ($C \cup T$) as expected. Also, in all distance comparison between pairs of breeds involving Duroc or Ghungroo, because of the lack of correlation between the feature sets (C) and (T); it has been observed that the feature set ($C \cup T$) does not provide the maximum distance between clusters with the exception of the Duroc-Yorkshire pair.

B. GUIDED TREE SELECTION

At a macro level, since a hierarchical classification strategy is to be adopted, based on the manner in which the training data is split and/or fused, for four breeds BR_i, BR_j, BR_k and BR_l, there are four distinct decision tree possibilities as shown in Fig. 13. The structure of the tree, which gives best classification results through a particular siphoning order at different

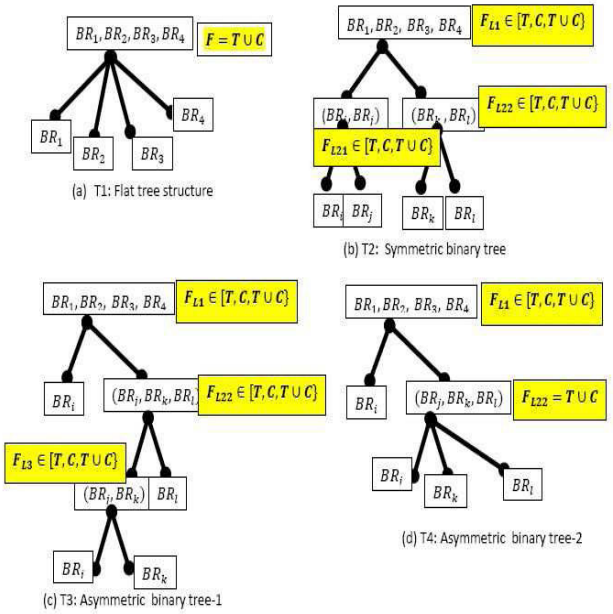

FIGURE 13. Classification routes or tree-types possible in a four class setting.

levels and with a proper feature choice (or choices) at those decision points, needs to be identified without going through the computational rigor. Given four breeds, Duroc (D), Ghungroo (G), Hampshire (H) and Yorkshire (Y) (which will eventually become four leaf nodes in the final decision tree), there are six pairwise breed-cluster distances that can be computed: (D-G), (D-H), (D-Y), (G-H), (G-Y) and (H-Y). There are three macro feature possibilities: (i) Colour feature alone (C); (ii) Texture feature alone (including GSM as well as Top-hat) (T); (iii) Union of Colour and Texture (Composite) ($T \cup C$). A sufficient set of distances which can be used to derive a strategy for breed-siphoning is the $6 \times 3 = 18$-cell table of breed-cluster pairwise-distances shown in Table. 6. From this Table. 6, secondary distances can be derived. To find out roughly how far each breed is cumulatively far away from the rest (with the same consistent rule), by pivoting around a specific breed, its distance from the other breeds are added up. This is in turn a function of the feature-type: Colour (C) or Texture (T) or Composite: Colour and Texture $C \cup T$.

The cumulative distance table (Table. 7) provides a distinct angular perspective from the point of view of the individual breeds. The separation of Duroc (D) from the remaining breeds is a function of the feature combination used: Turns out to be $S_{DUROC}(C) = 1.90 + 1.71 + 1.74 = 5.35$ with respect to colour; $S_{DUROC}(T) = 1.67 + 1.83 + 1.81 = 5.31$, with respect to texture and $S_{DUROC}(C, T) = 1.71 + 1.74 + 1.93 = 5.38$, with respect to the composite feature involving colour and texture. Similarly such statistics can be computed for the other three breeds leading to Table. 7. For a specific feature type (color or texture or UNION), if the deviation

TABLE 7. Cumulative distances with respect to a particular breed across various feature combinations.

BREED and feature	Colour	TEXTURE	Colour and TEXTURE
Duroc vs rest	5.35	5.31	5.38
Ghungroo vs rest	**5.81**	5.43	5.52
Hampshire vs rest	5.29	5.51	5.48
Yorkshire vs rest	5.35	5.63	5.74
CUMULATIVE-MAX	5.81	5.63	5.74
CUMULATIVE-MEDIAN	5.32	5.47	5.50
DIFF(MAX, MEDIAN)	**0.49**	0.16	0.24

TABLE 8. Leaving out Ghungroo, pairwise distances for various feature combinations, reproduced.

BREED and feature	D-H	D-Y	H-Y
C: Colour	1.71	1.74	1.64
T: Texture	**1.83**	1.81	1.87
$C \cup T$	1.74	**1.93**	**1.87**
Best features	T	$C \cup T$	$C \cup T$
MAX-distances	1.83	1.93	1.87

between the maximum cumulative distance and median is significant, this indicates a certain skew in the breed arrangement and also provides indirect information, that the optimal tree structure, may not be a flat tree (i.e. Fig. 13(a)). Here, from the scores, Table. 7, appears to indicate that Ghungroo should be siphoned out first, in terms of color and then the cumulative distance table should be recomputed without Ghungroo. If one compares the differential (MAX, MEDIAN) scores for color (0.49), texture (0.16) and UNION (0.24) from Table. 7, there is a hint that the color feature could be dominant over texture, for this specific 4-breed arrangement.

It is clear from the cumulative scores from Table. 7 that best results can be obtained from asymmetric binary split-tree types T3 (Fig. 13(c)) or T4 (Fig. 13(d)), where the solitary leaf node on the left happens to be Ghungroo (highest score) and the decision space is defined with respect the colour feature alone. Thus, the first level simplification results in a subtree (one versus three split), shown in Fig. 14. When the cumulative distances are recomputed (minus Ghungroo), one arrives at Table. 9 and from the deviation statistics, there is an indication that the tree structure is of type T3 (Fig. 13(c)) with the leaf being Yorkshire and the feature type being UNION of color and texture. Finally the tree structure converges to type T3 and the final tree is shown in Fig. 14. Note in the last leg since it is Duroc vs Hampshire, the feature is Texture (T), Table. 10, as the highest score is registered for T). As per the siphoning order in Fig. 14, Ghungroo is separated from the rest with respect to colour, Yorkshire versus the rest with respect to colour/texture and finally Hampshire is separated from Yorkshire with respect to texture alone.

V. CLASSIFICATION METHODS IN LITERATURE

A. PHYLOGENETIC ANALYSIS AND TREE CONSTRUCTION

The concept of constructing a Phylogenetic tree [30] based on the similarity and differences in the physical or genetic characteristics between different species to describe the evolutionary process, can also be used for arriving at the optimal

TABLE 9. Leaving out Ghungroo, cumulative distances with respect to a particular breed across various feature combinations.

BREED and feature	Colour	TEXTURE	Colour and TEXTURE
Duroc vs rest	3.45	3.64	3.67
Hamshire vs rest	3.35	3.70	3.61
Yorkshire vs rest	3.38	3.68	**3.80**
CUMULATIVE-MAX	3.45	3.70	3.80
CUMULATIVE-MEDIAN	3.38	3.68	3.67
DIFF(MAX, MEDIAN)	0.07	0.02	0.13

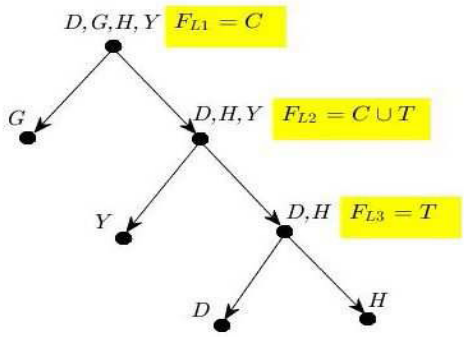

FIGURE 14. Final decision tree and siphoning policy.

TABLE 10. Leaving out Ghungroo and Yorkshire, pairwise distances for various feature combinations reproduced.

BREED and feature	D-H
C: Colour	1.71
T: Texture	**1.83**
$T \cup C$	1.74
Best features	T
MAX-distances	1.83

classification hierarchy. Given required information regarding breeds, the methods for the construction of this optimal phylogenetic tree can be classified mainly into three categories: (i) Distance based methods [31]: These methods are used when pairwise distances between the different entities are available for the construction of the phylogenetic tree. Each leaf node on the phylogenetic tree represents one entity. A hierarchical clustering algorithm is used for preserving the relative distance between different entities on the tree; (ii) Maximum parsimony [32]: This method searches for the phylogenetic tree with the minimum number of evolutionary steps which can explain a given set of data assigned on the leaves. Here, the topology of the tree is randomly changed till there is no more improvement in the parsimony; (iii) Likelihood-based methods [33]: This method involves computing the likelihood of the given data sequence with standard evolution models and the tree corresponding to the best likelihood model is generated.

The requirement in all cases is to identify a tree which can maximize the separation between the child nodes at each step of evolution, so that the best classification accuracy is possible with the given set of features. Distance based methods using hierarchical clustering algorithms [34] are the best choice since they try to separate out the maximally distant classes at each step of evolution starting from the root node. Thus in the first stage the class which is farthest from all the other classes is separated out; in the second stage, out of the remaining classes, the one which is farthest from the remaining others is separated out and so on. The Bioinformatics Toolbox in MATLAB [35] provides functions related to Phylogenetic analysis using Distance based methods. The function takes the matrix of pairwise distances and uses a Hierarchical Agglomerative Nesting algorithm (AGNES) [34] to cluster objects based on their similarity. The algorithm starts by treating each object (breed) as a singleton cluster. Next, pairs of clusters are successively merged until all clusters have been merged into one big cluster containing all objects. The result is a tree-based representation of the objects, named *Dendrogram*, where the leaf-nodes correspond to the breed-types. At each step of the algorithm, the two clusters that are the most similar are combined into a new bigger cluster (nodes). This procedure is iterated until all points are member of just one single big cluster (root).

The process does not however prescribe a procedure for arriving at the right choice of features/statistics at each decision point (i.e. is feature agnostic) and also handling multiple features. If the matrix of pairwise distances is created by selecting the branch weight between any two breeds as the maximum distance over all the feature combinations for that breed-pair, then a tree can be constructed (even this feature is not available with the AGNES). The final phylogenetic tree which is built on this collection of maximal distances, remains therefore completely *feature type agnostic*. The AGNES therefore demands some form of a higher level protocol, first, to generate a distance table based on some fusion measure and then to identify the best feature at various levels in the tree.

B. DECISION TREES

Decision trees [36] though being very simple machine learning techniques have the powerful property of being able to automatically select the attributes from the feature vector which can impart maximum separation between two or more classes of data given the training samples. Starting from the root node, each parent node is split into multiple child nodes in a way that the purity of each child node is maximized. The most widely used splitting criterion are based on Gini's Diversity Index [37] and entropy reduction methods [38]; although more recent methods are available in literature for binary [39] and non-binary splits [40] which ensure the constructed tree is more compact with smaller number of nodes without compromising on the classification accuracy. The major steps involved in the construction of a decision tree include: (i) Selecting one of the attributes(a_i) from the feature vector; (ii) Choosing a threshold(t_i) for that attribute, that divides the training data into child nodes; (iii) Measuring purity of the child nodes, when the parent node is split based on the attribute a_i using the threshold t_i (iv) Repeating this process for all the attributes and feasible t_i till maximum purity is obtained, for all the child nodes (v) On obtaining the maximum purity split, the process is repeated for a second

split, and so on. The following are some issues which can be anticipated with this decision tree approach:

- Attribute selection is not the same as feature-type selection, as the selection is done by randomly sampling the parent composite feature set. Since this random attribute selection design is not in tune with the on-field analysis and customization, results are definitely expected to be poorer as compared to the optimal hierarchical tree generation algorithm (which includes feature-type identification).
- While decision trees are expected to work well with raw data vectors and simple primary statistics, performance will degrade when the feature vectors include secondary and robust statistics, which are compact in nature. Decimation of such secondary statistics is expected to result in an information loss both with respect to within-class similarity (which brings breed-specific variants together) with respect to that parameter (which has been dropped), as well as precious information which imparts segregation across breeds. For instance dropping the bi-modality index will make Hamshire pigs look like Yorkshire (with respect to colour).

VI. EXPERIMENTAL RESULTS AND COMPARISONS

A. DATABASE AND TRAINING/TESTING PROCEDURE

The dataset used for the experiments consists of a total of 673 images for 55 animals taken from all the 4 breeds. Out of these 55 animals, 11 belonged to Duroc, 13 belonged to Ghungroo, 12 to Hampshire and 19 to Yorkshire. Thus on an average there were 12 images for each animal and these different images of the same pig shows the variation caused due to camera pan, skew effects and blur. 50% of the data was used for training and the remaining 50% for testing. This is a form of cross-testing, as the pigs used for testing are completely different from the pigs used for learning and generating the tree-classifier model (coupled with the optimal choice of features). For image acquisition, a high resolution digital camera was used. The images were cropped manually to suppress extreme background interference. But despite this we had to put these images through a level of automated segmentation, via a circular mask BALL-generation procedure to highlight portions only on the muzzle surface.

B. PERFORMANCE EVALUATION FOR THE FLAT TREE

The formation of a decision policy to establish the optimal hierarchical scheme for classification is of paramount importance. The results for a 4-class linear classifier, are tabulated in Table 11. The mean and the standard deviation of the classification accuracies for 100 iterations are given for each of the three feature types.

Table. 11, shows that Yorkshire and Ghungroo have registered the highest numbers 98.22% and 92.38%, respectively with respect to the composite (both colour and texture features), since, they are both distinct in terms of colour (Yorkshire all pinkish-white muzzle and Ghungroo is all greyish-black). This can be corroborated by the corresponding ''Colour only'' feature scores of 95.44% and 89.80% respectively (same Table. 11). The drop takes place with respect to ''Texture only'', for Ghungroo as it shares similar patch density profiles with Duroc and Hampshire (Ghungroo's classification accuracy drops to 65.97% for texture alone, while for Yorkshire it remains high at 96.49%). Since the pigs used for training and testing were completely different, the testing process was tough as the pigs exhibited considerable variability on the following fronts:

(i) Hair and pore density profiles: type, location and concentration of patterns was completely different for different pigs within the same breed; (ii) Breeds like Duroc and Hampshire which were expected to have pinkish-white patches on their muzzle, exhibited considerable unpredictability in the size, position and structure of the patch on the muzzle surface for the pigs being tested for the first time; (iii) These pigs being tested also exhibited differential variability with respect to local illumination and environmental settings.

TABLE 11. Table showing the mean percentage accuracy for 100 iterations for the proposed colour, texture and combined features. A Flat Tree structure was deployed (i.e. linear classifier for a 4-class SVM).

	Colour		Texture		Combined	
	Mean	St.Dev	Mean	St.Dev	Mean	St.Dev
Duroc	68.14	21.80	51.88	18.00	84.00	13.85
Ghungroo	89.80	10.43	65.97	15.86	92.38	9.42
Hampshire	73.81	13.94	84.40	10.32	81.62	9.98
Yorkshire	95.44	6.13	96.49	2.97	98.22	3.57

C. PERFORMANCE EVALUATION: PROPOSED TREE STRUCTURE

The training and testing image subsets were randomly selected and the process was iterated 10 or more times to investigate the impact of training data variability on the final classification accuracies. At the beginning of each iteration, the training process involved computation of the features for those images and determining the optimal hierarchical structure (based on the algorithm in Section. IV) from the cluster/breed distances. Using the labeled features from the same training-arrangement, SVM classifiers were learnt for all the three stages of classification, identified by the feature type selection procedure. This random train-test splitting process was repeated multiple times. The hierarchy/TREE, obtained from the training data in all the 10 iterations, wherein the training and test sets were split randomly (to check tree stability), turned out nearly the same as shown in Table. 12, which indicated two things: (i) Tree structure was relatively insensitive to changes in the cross-validation arrangements during the train-test iterations, wherein 50% of the pigs were randomly picked for training and the other 50% were short-listed for testing. Table. 12, shows the hierarchies obtained using the proposed algorithm for all the ten iterations. For seven out of ten (7/10) cases, the tree had the same structure: $G-Y-(D,H)$ (i.e. the breeds as leaf nodes were picked out in the order: Ghungroo, Yorkshire, and then finally Hampshire versus Duroc). (ii) The secondary features covering both

TABLE 12. Hierarchy obtained along with accuracies using the proposed algorithm for the same 10 random selections of training data as used in Table 15 along with the feature choice at each node.

Iteration	Linked List	MAX-L1/ $\mathbf{F}_{L1}$	MAX-L2/ $\mathbf{F}_{L2}$	MAX-L3/ $\mathbf{F}_{L3}$	Duroc Accuracy(%)	Ghungroo Accuracy(%)	Hampshire Accuracy(%)	Yorkshire Accuracy(%)
TREE-1	G-Y-(D,H)	5.82/C	3.81/(C,T)	1.8/T	91.12	93.52	86.71	96.23
TREE-2	G-Y-(D,H)	5.81/C	3.78/(C,T)	1.83/T	84.31	90.29	84.23	98.17
TREE-3	G-Y-(D,H)	5.77/C	3.8/(C,T)	1.77/T	76.23	87.32	78.55	96.78
TREE-4	G-Y-(D,H)	5.81/C	3.81/(C,T)	1.83/T	81.48	91.63	87.21	99.54
TREE-5	G-Y-(D,H)	5.83/C	3.77/(C,T)	1.79/T	88.45	94.79	80.48	100.00
TREE-6	Y-G-(D,H)	5.79/(C,T)	3.74/C	1.81/T	79.47	96.53	83.65	95.41
TREE-7	G-Y-(D,H)	5.8/C	3.79/(C,T)	1.82/T	80.45	89.41	90.32	99.54
TREE-8	G-Y-(D,H)	5.85/C	3.8/(C,T)	1.78/T	83.78	97.13	81.68	100.00
TREE-9	G-Y-(D,H)	5.77/C	3.82/(C,T)	1.82/T	77.21	86.33	92.57	100.00
TREE-10	Y-H-(D,G)	5.82/(C,T)	3.64/C	1.88/C	77.42	89.79	84.22	100

TABLE 13. Classification accuracy (100 iterations), following the TREE hierarchy obtained, using our method.

	Mean	St.Dev
Duroc	86.45	12.05
Ghungroo	93.02	7.46
Hampshire	86.91	12.51
Yorkshire	98.54	4.84

TABLE 14. Confusion matrix for proposed tree algorithm.

Actual \ Predicted	Duroc	Ghungroo	Hampshire	Yorkshire
Duroc	56	5	3	1
Ghungroo	4	70	1	0
Hampshire	6	2	60	1
Yorkshire	0	1	1	108

texture and colour were robust for trapping breed-specific traits while dissolving individual variability within the same breed.

Table 13, shows classification accuracies with respect to the stable hierarchical scheme described in Section. IV and shown in Fig. 14. In relation to the flat-tree (four-class) arrangement, the proposed TREE registered a higher score of 86.45% versus 84.00% for Duroc; 93.02% versus 92.38% for Ghungroo; 86.91% versus 81.62% for Hampshire and 98.54% versus 98.22% for Yorkshire; The main improvement was in the score for Hampshire (one of the toughest breeds for classification which exhibited a similarity in texture profile with respect to both Duroc and Ghungroo and also a similarity in colour with respect to Duroc). The improvement for Hampshire, stemmed from the fact that Ghungroo taken out earlier in the TREE arrangement, comparison could now be done exclusively on the texture front (ignoring the color profile).

The corresponding confusion matrix is shown in Table 14. The first row of the confusion matrix tabulates the number of actual Duroc muzzle images being classified as one of the four breeds. The second row gives the same numbers for the actual Ghungroo muzzle images. In the same way the third row corresponds to Hampshire and the fourth row to Yorkshire. Ideally the confusion matrix should have been a diagonal matrix with all the non-diagonal elements equal to zero. However, because of some mis-classification between the breeds, the matrix is not a diagonal one. From the first row of this confusion matrix, it can be observed that Duroc has the maximum confusion with Ghungroo on account of its moderate to high density of hair follicles and pores on the muzzle surface. This same reason applies to some of Ghungroo muzzle images being confused with Duroc muzzle images as observed from the first entry in second row. Also, it can be observed from Table 14 that there is some confusion between Duroc and Hampshire as well. This is because there is some similarity in the density profile of hair follicles and pores present on the muzzle surface of both the breeds. Also some of the Duroc breeds have a significant pinkish white patch on their muzzle which is mainly a characteristic of Hampshire breed and this becomes a source of confusion between the two breeds.

D. COMPARISON WITH THE PHYLOGENETIC TREE ALGORITHM (AGNES)

Table. 15, shows the hierarchies obtained from the Phylogenetic tree algorithm [34] used by the Phylogenetic MATLAB Toolbox [35] for 10 different random splits of training-testing data (50%-50%). The training-testing data used in the 10 iterations are the same as those used for evaluating the results in Table 12. While the Phylogenetic algorithm processes the breed-pair distance Table. 6, it is *feature agnostic*. It does not provide a mechanism for arriving at or selecting the optimal combination of features for forming the decision space at every intermediate node. Hence, for comparison purposes each of the node in the linked list has been supplied with the feature set $(C \cup T)$. Fig. 15, shows a typical tree produced by the AGNES MATLAB toolbox corresponding to the first row of Table. 15. The Phylogenetic tree structure (unlike the proposed algorithm) exhibits a high variability or data-sensitivity (four instances of TREE: $Y - G - (D, H)$; two instances of $G - Y - (D, H)$; two instances of $Y - H - (D, G)$ and two instances of $Y - D - (G, H)$) (Table. 15). In contrast, the proposed algorithm showed a strong base tree $G - Y - (D, H)$, which remained virtually the same (8 out of 10 times) for the same database-splits, identical to the proposed optimal tree in Fig. 12. Mean accuracies for AGNES toolbox are in Table. 16 based on the tree structure $Y - G - (D, H)$ (Yorkshire first and then Ghungroo, the main difference; last stage same, for both proposed and AGNES). Accuracies for

TABLE 15. Table showing the hierarchies obtained from the AGNES algorithm used by the Phylogenetic Toolbox for the same 10 different random splits of training-testing data (50%-50%) as used in Table 12. Feature used at each node of hierarchy is $C \cup T$.

Iteration	Linked List	Duroc Accuracy(%)	Ghungroo Accuracy(%)	Hampshire Accuracy(%)	Yorkshire Accuracy(%)
TREE-1	Y-G-(D,H)	76.15	98.58	80.53	97.88
TREE-2	Y-D-(G,H)	83.21	90.22	75.48	97.34
TREE-3	G-Y-(D,H)	82.63	87.42	78.39	98.32
TREE-4	Y-G-(D,H)	80.51	89.78	77.24	100.00
TREE-5	G-Y-(D,H)	79.42	93.21	82.38	100
TREE-6	Y-H-(D,G)	85.43	92.19	84.71	97.23
TREE-7	Y-D-(G,H)	74.44	92.64	83.19	98.56
TREE-8	Y-G-(D,H)	77.83	90.19	76.22	100.00
TREE-9	Y-H-(D,G)	74.31	94.39	83.78	100.00
TREE-10	Y-G-(D,H)	86.48	100.00	82.64	99.14

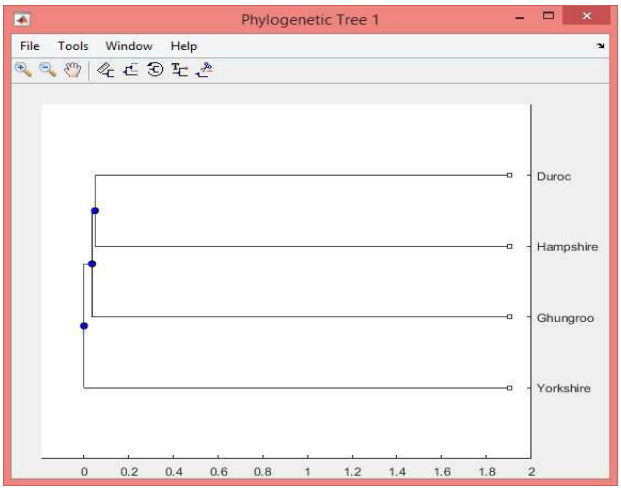

FIGURE 15. AGNES TREE-1.

TABLE 16. Accuracies obtained using the feature agnostic, Phylogenetic toolbox (features selected using the procedure from sub-section IV-B) and the mean tree $Y - G - (D, H)$ (Table. 15).

	Mean	St.Dev
Duroc	83.58	15.11
Ghungroo	94.11	9.07
Hampshire	81.78	11.92
Yorkshire	96.19	3.28

Duroc, Hampshire and Yorkshire were on the lower side for AGNES, registering 83.58%,81.78% and 96.19% respectively. In contrast, the proposed TREE registered higher scores, 86.45%,and 86.91% for the critical/difficult breeds, Duroc and Hampshire respectively.

E. COMPARISON WITH DECISION TREES

Decision trees are useful when one is operating on raw measurements, as opposed to handcrafted statistics and work via random attribute sampling, to identify the decision space where the separation between sub-groups of data is maximized. While the tree search is extensive, there are several reasons why this route turns out to be sub-optimal: (i) When features are handcrafted, they cannot be selectively dropped on a random basis, as every single statistic plays a crucial role towards breed separation. Deleting some of them from the decision making procedure or de-registering the feature vectors through random sampling, will only degrade the overall performance; (ii) Attributes when mixed as a union of colour and texture assume a "colourless" flavor, wherein no attribute is pre-labeled. No knowledge gained from the colour or texture feature analysis is used in the attribute search and sub-sampling procedure. In compact feature vectors, when tailor-made statistics such as the Sarle's bi-modality index [10] and the chromatic eigen value ratio, are randomly dropped from the (colour, texture) feature mixture, performance degradation is expected (as can be seen in Table. 17). Not surprisingly, the accuracies for Duroc, Ghungroo and Hampshire have dropped below 80%.

TABLE 17. Breed accuracies obtained using the decision tree architecture.

	Mean	St.Dev
Duroc	73.81	20.50
Ghungroo	75.78	17.76
Hampshire	71.42	14.84
Yorkshire	92.07	6.87

F. ABSENCE OF SEGMENTATION AND OVERALL PICTURE

The proposed BALL-based muzzle segmentation process, described in Section. II, ensures that colour and texture features are not affected by the portion outside the muzzle region. Comparisons between the proposed and classification algorithms from literature, in terms of accuracies, are now re-evaluated both with and without the mask. Table. 18 shows a reduction in the accuracies for the tree-based algorithms (including both proposed and the ones from literature), in the absence of segmentation. Note that interestingly the background profiles for different breeds are heavily pig-specific, as the background interference usually arises from two sides: (i) Face of the pig and (ii) In some cases, glove of the individual clutching the pig's snout. The fractional background portion outside the muzzle region constitutes roughly 25% of the total cropped square area. This background composition (25%) varies from pig to pig (even within the same breed), and creates an inconsistency in the breed-linked feature modeling procedure. The impact of our BALL-based segmentation algorithm on the classification accuracy, is checked and compared with the accuracies obtained by applying masks using the Chan-Vese [16], DRLSE [15], SDREL [20], active contour models (in Table 19). Clear evidence of the

TABLE 18. Accuracies for proposed tree, AGNES and decision trees (NO segmentation).

	Proposed Tree		Phylo Tree		Decision Tree	
	Mean	St.Dev	Mean	St.Dev	Mean	St.Dev
Duroc	64.73	17.07	62.23	14.48	52.97	17.23
Ghungroo	81.78	13.39	79.50	17.76	69.38	17.89
Hampshire	80.77	11.23	80.96	8.02	66.71	18.30
Yorkshire	96.78	3.77	96.13	4.87	91.66	10.14

TABLE 19. Accuracies, with segmentation, using a variety of methods and comparison with proposed BALL-based approach (Difficulty level maximum for Hampshire breed).

	Proposed BALL-method		DRLSE		SDREL		Chan-Vese		NO segmentation	
	Mean	St.Dev	Mean	St.Dev	Mean	St.Dev	Mean	St.Dev	Mean	St.Dev
Duroc	86.45	12.05	80.29	9.72	66.33	18.37	51.72	19.34	64.73	17.07
Ghungroo	93.02	7.46	85.11	17.17	82.77	11.17	91.05	6.72	81.78	13.39
Hampshire	86.91	12.51	81.72	10.18	59.13	16.40	40.63	14.36	80.77	11.23
Yorkshire	98.54	4.84	93.68	4.84	95.11	6.39	87.10	9.30	96.78	3.77

superiority of the proposed BALL based segmentation conjecture, can be seen from the classification results, particularly for Hampshire, where the muzzle profile exhibits color diversity in a dual mode (i.e. pink and grey).

VII. CONCLUSION AND DISCUSSIONS

In this paper, the focus was on qualifying the muzzle of a pig as a robust breed descriptor. Since the available methods in literature related to breed classification in animals based on visual biometrics uses Deep Neural Networks [7], [8], a direct technology transfer is not possible in this case due to the availability of very limited data. Apart from developing a segmentation procedure for picking out the internal details of the muzzle, visual descriptors for computing the feature vectors were identified. Based on the observations in Table 1, customized descriptors had to be designed on two fronts: Colour and Texture descriptors. (i) Color descriptors are based on statistics from the 2D-colour histogram in the $C_b - C_r$ space, such as eigenvalue ratios, means, moments and most importantly the Sarle's Bi-modality index; (ii) On the texture front, two gradient operators: GSM and Top-hat, were used to filter the muzzle profiles separately and the results were later quantized to obtain two binary maps. Subsequently the feature vectors were extracted from these quantized binary maps. Since the four breeds could not be separated well enough using a single classifier and a single feature type as can be observed from the classification accuracies in Table 11; hence a hierarchical classification scheme had to be adopted.

To decide the classification tree structure and breed siphoning order along with the feature type: (C),(T) or $C \cup T$, a tree synthesis algorithm was designed to feed on a pairwise breed/cluster distance table generated from the training set. Training and testing was done on completely different pigs and these train-test splits were randomized to check stability of the final siphoning order (or the mean TREE). The proposed tree algorithm out-performed both the feature agnostic AGNES-architecture (phylogenetic toolbox) as well as the attribute sampling driven decision tree algorithm as can be inferred from the accuracies reported in Table 16 and Table 17. AGNES demonstrated a tree-instability and being feature agnostic, had to be fed with feature-types by analysing the breed-distance table. The importance of muzzle segmentation prior to feature extraction, can be well understood from the results in Table 18. Performance improvement of the proposed segmentation technique, i.e. adaptive ball fitting procedure, with the help of the directional Gabor-triad filter, with respect to the other state of the art segmentation techniques is presented in Table 19. The proposed algorithm reported relatively high mean accuracies of 86.45% for Duroc, 93.02% for Ghungroo, 86.91% for Hampshire and 98.54% for Yorkshire.

This work provides fairly strong evidence regarding the utility of the muzzle image of a pig as a potential pig breed identifier and can be extended further in the future with more number of breeds to further strengthen this hypothesis. Although the proposed segmentation algorithm is customized, it can still be used in segmentation tasks where the location of the contour defining the boundary of the object is approximately known; but is complex and partially diffused.

The proposed tree synthesis procedure searches for a bias with respect to a specific breed (some breeds such as Ghungroo and Yorkshire are easier to pick out of the mixture) and chalks out, not just the selection order, but also the best choice of feature, at each intermediate decision point. Hence, this tree synthesis process, with many more secondary statistics and guidelines, can be extended to attack a larger frame comprising of n classes, m basic feature types (m small), purely based on the pairwise distance table which will now have $O(2^m \times n^2)$ entries. The main weakness is that the current set of guidelines for tree-synthesis (based on cumulative, feature specific distance statistics) are fairly simplistic and effective for both small n (classes/breeds) and small m (basic feature types). For a larger arrangement, say large scale dog breed classification problem, based on facial images (large n and moderate m), one will require more sophisticated protocols and guidelines for intermediate decision making and feature selection.

ACKNOWLEDGMENT

This work is a byproduct of an IMAGE IDGP sub-project, under the purview of a broader initiative, related to Identification, Tracking and Epidemiological analysis of pigs and goats. This comes under the ITRA frame, which is a national level research initiative controlled and sponsored by the Ministry of Information Technology, Government of India. The authors thank Dr. Santanu Banik and his ICAR RANI team (Rani, Guwahati, Assam) for collaborating with us [the signal processing partners from IIT Guwahati] and for capturing samples of Annotated Muzzle Images from the ICAR Rani pig farm, which eventually formed the repository for the breed analysis.

REFERENCES

[1] C. Cai and J. Li, "Cattle face recognition using local binary pattern descriptor," in *Proc. Asia–Pacific Signal Inf. Process. Assoc. Annu. Summit Conf.*, Oct. 2013, pp. 1–4.

[2] K. Karthik, S. Chakraborty, and S. Banik, "Muzzle analysis for biometric identification of pigs," in *Proc. 9th Int. Conf. Adv. Pattern Recognit. (ICAPR)*, Dec. 2017, pp. 1–6.

[3] P. Chetia. (2020). *High Milk Producing Indian Cattle Breed: These 4 Indian Breed Can Give Milk up to 80 Liters*. [Online]. Available: https://krishijagran.com/animal-husbandry/high-milk-producing-indian-cattle-breed-these-4-indian-breed-can-give-milk-up-to-80-liters/

[4] S. Kadam. *Imported Breeds of Pig Used in India*. [Online]. Available: https://www.notesonzoology.com/india/pig-farming/imported-breeds-of-pig-used-in-india/1296

[5] S. Chakraborty, K. Karthik, and S. Banik, "Investigation on the muzzle of a pig as a biometric for breed identification," in *Proc. 3rd Int. Conf. Comput. Vis. Image Process.* Singapore: Springer, 2020, pp. 71–83. [Online]. Available: https://www.springerprofessional.de/en/investigation-on-the-muzzle-of-a-pig-as-a-biometric-for-breed-id/17338414

[6] I. P. F. Wayne, I. D. C. P. Rusk, and I. D. B. T. Richert, "Identification of swine by auricular vein patterns," Tech. Rep., 1986. [Online]. Available: http://citeseerx.ist.psu.edu/viewdoc/download?doi=10.1.1.504.7542&rep=rep1&type=pdf, doi: 10.1.1.504.7542.

[7] Z. Raduly, C. Sulyok, Z. Vadaszi, and A. Zolde, "Dog breed identification using deep learning," in *Proc. IEEE 16th Int. Symp. Intell. Syst. Informat. (SISY)*, Sep. 2018, pp. 271–276.

[8] R. Kumar, M. Sharma, K. Dhawale, and G. Singal, "Identification of dog breeds using deep learning," in *Proc. IEEE 9th Int. Conf. Adv. Comput. (IACC)*, Dec. 2019, pp. 193–198.

[9] A. K. Jain and F. Farrokhnia, "Unsupervised texture segmentation using Gabor filters," *Pattern Recognit.*, vol. 24, no. 12, pp. 1167–1186, 1991.

[10] R. Pfister, K. A. Schwarz, M. Janczyk, R. Dale, and J. B. Freeman, "Good things peak in pairs: A note on the bimodality coefficient," *Frontiers Psychol.*, vol. 4, p. 700, Oct. 2013.

[11] PorkmoneyBlog. (2019). *Pig Snouts: All You Need to Know About Their Importance and Uses*. [Online]. Available: https://www.porkmoney.com/blog/2019/07/05/pig-snouts-all-you-need-to-know-about-their-importance-and-uses/

[12] W. Xun, L. Shi, H. Zhou, G. Hou, and T. Cao, "Effect of weaning age on intestinal mucosal morphology, permeability, gene expression of tight junction proteins, cytokines and secretory IgA in Wuzhishan mini piglets," *Italian J. Animal Sci.*, vol. 17, no. 4, pp. 976–983, Oct. 2018.

[13] E. Iqbal, A. Niaz, A. A. Memon, U. Asim, and K. N. Choi, "Saliency-driven active contour model for image segmentation," *IEEE Access*, vol. 8, pp. 208978–208991, 2020.

[14] A. Munir, S. Soomro, M. T. Shahid, T. A. Soomro, and K. N. Choi, "Hybrid active contours driven by edge and region fitting energies based on p-Laplace equation," *IEEE Access*, vol. 7, pp. 135399–135412, 2019.

[15] C. Li, C. Xu, C. Gui, and M. D. Fox, "Distance regularized level set evolution and its application to image segmentation," *IEEE Trans. Image Process.*, vol. 19, no. 12, pp. 3243–3254, Dec. 2010.

[16] T. F. Chan and L. A. Vese, "Active contours without edges," *IEEE Trans. Image Process.*, vol. 10, no. 2, pp. 266–277, Feb. 2001.

[17] L. Wang, J. Zhu, M. Sheng, A. Cribb, S. Zhu, and J. Pu, "Simultaneous segmentation and bias field estimation using local fitted images," *Pattern Recognit.*, vol. 74, pp. 145–155, Feb. 2018.

[18] X.-F. Wang, D.-S. Huang, and H. Xu, "An efficient local Chan–Vese model for image segmentation," *Pattern Recognit.*, vol. 43, no. 3, pp. 603–618, 2010.

[19] Q. Cai, H. Liu, Y. Qian, S. Zhou, X. Duan, and Y.-H. Yang, "Saliency-guided level set model for automatic object segmentation," *Pattern Recognit.*, vol. 93, pp. 147–163, Sep. 2019.

[20] X.-H. Zhi and H.-B. Shen, "Saliency driven region-edge-based top down level set evolution reveals the asynchronous focus in image segmentation," *Pattern Recognit.*, vol. 80, pp. 241–255, Aug. 2018.

[21] Y. Zhang, W. Li, L. Zhang, X. Ning, L. Sun, and Y. Lu, "Adaptive learning Gabor filter for finger-vein recognition," *IEEE Access*, vol. 7, pp. 159821–159830, 2019.

[22] X. Wang, W. Du, F. Guo, and S. Hu, "Leaf recognition based on elliptical half Gabor and maximum gap local line direction pattern," *IEEE Access*, vol. 8, pp. 39175–39183, 2020.

[23] P. Sebastian, Y. V. Voon, and R. Comley, "The effect of colour space on tracking robustness," in *Proc. 3rd IEEE Conf. Ind. Electron. Appl.*, Jun. 2008, pp. 2512–2516.

[24] R. C. Gonzalez, R. E. Woods, and S. L. Eddins, *Digital Image Processing Using MATLAB*. London, U.K.: Pearson, 2004.

[25] T. Chen, Q. Wu, R. Rahmani-Torkaman, and J. Hughes, "A pseudo top-hat mathematical morphological approach to edge detection in dark regions," *Pattern Recognit.*, vol. 35, no. 1, pp. 199–210, 2002.

[26] T. R. Knapp, "Bimodality revisited," *J. Mod. Appl. Stat. Methods*, vol. 6, no. 1, pp. 8–20, May 2007.

[27] L. V. D. Maaten and G. Hinton, "Visualizing data using t-SNE," *J. Mach. Learn. Res.*, vol. 9, pp. 2579–2605, Nov. 2008.

[28] L. Armi and S. Fekri-Ershad, "Texture image analysis and texture classification methods—A review," 2019, *arXiv:1904.06554*. [Online]. Available: http://arxiv.org/abs/1904.06554

[29] R. De Maesschalck, D. Jouan-Rimbaud, and D. L. Massart, "The Mahalanobis distance," *Chemometrics Intell. Lab. Syst.*, vol. 50, no. 1, pp. 1–18, 2000.

[30] L. L. Cavalli-Sforza and A. W. Edwards, "Phylogenetic analysis. models and estimation procedures," *Amer. J. Hum. Genet.*, vol. 19, nos. 1-3, p. 233, 1967.

[31] W. H. Li, "Simple method for constructing phylogenetic trees from distance matrices," *Proc. Nat. Acad. Sci. USA*, vol. 78, no. 2, pp. 1085–1089, Feb. 1981.

[32] L. Kannan and W. C. Wheeler, "Maximum parsimony on phylogenetic networks," *Algorithms Mol. Biol.*, vol. 7, no. 1, p. 9, Dec. 2012.

[33] NCBI. (2004). *Maximum Likelihood*. [Online]. Available: https://www.ncbi.nlm.nih.gov/Class/NAWBIS/Modules/Phylogenetics/phylo15.html

[34] L. Kaufman and P. J. Rousseeuw, *Finding Groups Data: Introduction to Cluster Analysis*, vol. 344. Hoboken, NJ, USA: Wiley, 2009.

[35] R. Henson and L. Cetto, *The MATLAB Bioinformatics Toolbox*. Hoboken, NJ, USA: Wiley, 2005. [Online]. Available: https://onlinelibrary.wiley.com/doi/10.1002/047001153X.g409308

[36] L. Breiman, J. Friedman, C. J. Stone, and R. A. Olshen, *Classification Regression Trees*. Boca Raton, FL, USA: CRC Press, 1984.

[37] W.-Y. Loh and Y.-S. Shih, "Split selection methods for classification trees," *Statistica Sinica*, vol. 5, pp. 815–840, Oct. 1997.

[38] J. R. Quinlan, "Improved use of continuous attributes in C4.5," *J. Artif. Intell. Res.*, vol. 4, pp. 77–90, Mar. 1996.

[39] F. Wang, Q. Wang, F. Nie, Z. Li, W. Yu, and F. Ren, "A linear multivariate binary decision tree classifier based on K-means splitting," *Pattern Recognit.*, vol. 107, Nov. 2020, Art. no. 107521.

[40] B. Chandra, R. Kothari, and P. Paul, "A new node splitting measure for decision tree construction," *Pattern Recognit.*, vol. 43, no. 8, pp. 2725–2731, 2010.

SHOUBHIK CHAKRABORTY is currently pursuing the Ph.D. degree with the EEE Department, Indian Institute of Technology, Guwahati, India. His research interests include computer vision and machine learning.

KANNAN KARTHIK received the Ph.D. degree from the University of Toronto, Canada, in 2006. He is currently an Associate Professor with the Indian Institute of Technology, Guwahati, India. His research interests include privacy preserving multimedia processing, access control, and biometric counter-spoofing.

SANTANU BANIK received the Ph.D. degree in animal genetics and breeding from the National Dairy Research Institute, Karnal, India, in 2004. He is currently a Senior Scientist at ICAR-National Research Center on Pigs. His research interests include in the evaluation, characterization, and conservation of indigenous pig germ-plasm, development of crossbred pig varieties, and image-based identification of individual/breed through IT interventions.